Marine Geology 242 (2007) 83 – 108
MARINE GEOLOGY
INTERNATIONAL JOURNAL OF MARINE GEOLOGY, GEOCHEMISTRY AND GEOPHYSICS
www.elsevier.com/locate/margeo

Holocene sedimentary evolution and palaeocoastlines of the Lower Khuzestan plain (southwest Iran)

Vanessa Mary An Heyvaert [a,b,*], Cecile Baeteman [a]

[a] Geological Survey of Belgium, Royal Belgian Institute for Natural Sciences, Jennerstraat 13, 1000 Brussels, Belgium
[b] Department of Geology, Vrije Universiteit Brussel, 1000 Brussels, Belgium

Received 4 May 2006; received in revised form 10 January 2007; accepted 26 January 2007

Abstract

The Holocene sequence of the Lower Khuzestan plain in southwest Iran has been investigated in the context of coastal evolution and relative sea-level change. A literature review about the coastal evolution of the Shatt-el Arab region with respect to relative sea-level changes is provided. The sedimentary succession in undisturbed hand-operated cores and temporary outcrops is described and facies are identified on the basis of lithology, sedimentary structures and macrofossils. Four main sedimentary environments are interpreted from the Holocene sedimentary record of the plain: brackish tidal flat, clastic coastal sabkha, brackish–freshwater marsh and fluvial plain. The study of the vertical and spatial distribution of sedimentary facies, their environmental interpretation especially with respect to the relationship to tide levels is done for five different zones in the plain. Chronological control is provided by radiocarbon dates. On the basis of this analysis, palaeogeographical reconstructions of the Lower Khuzestan plain, and the northern extension of the Persian Gulf were made for different points in time between 8000 and 450 cal BP. This study shows that during the early and middle Holocene, the Lower Khuzestan plain was a low-energy tidal embayment under estuarine conditions. During the initial sea-level rise of the early Holocene, the coastline rapidly transgressed across the shelf, and drowning of a major valley resulted in the development of extended tidal flats. Deceleration of sea-level rise after approximately 5500 cal BP, together with probably more arid conditions, allowed coastal sabkhas to extend widely and to aggrade while the position of the coastline remained relatively stable. Continued deceleration of sea-level rise initiated the progradation of the coastline from ca. 2500 cal BP. The effect of sediment supply by the rivers became more important than the effect of relative sea-level rise. The Karun megafan developed under a descelerating rate of sea-level rise, controlling the avulsive shifting of the rivers Karkheh and Jarrahi and their loci of sediment input. Moreover, in this study it is suggested that a Holocene RSL highstand, above the present-day sea level, as suggested by previous workers, did not occur.

Keywords: Persian Gulf; relative sea-level change; lithological facies analyses; tidal environments; palaeogeography

1. Introduction

The Lower Khuzestan plain, located in southwestern Iran, forms the southeastern extension of the Lower Mesopotamian plain. It borders to the west one of the most important estuaries of the Middle-east region, i.e. the Shatt-el Arab. Three major rivers (Tigris, Euphrates

* Corresponding author. Geological Survey of Belgium, Royal Belgian Institute for Natural Sciences, Jennerstraat 13, 1000 Brussels, Belgium. Tel.: +32 27887651; fax: +32 26477359.
E-mail address: vanessa.heyvaert@naturalsciences.be (V.M.A. Heyvaert).

0025-3227/$ - see front matter
doi:10.1016/j.margeo.2007.01.008

and Karun) flow into the Shatt-el Arab which debouches into the Persian Gulf nearby Fao (Fig. 1).

According to literature the Shatt-el Arab/Tigris–Euphrates–Karun region was subjected to an extensive marine transgression in the middle and late Holocene, resulting in a shoreline far north of its present position, in response to rapid sea-level rise, followed by a delta progradation due to eustatic sea-level changes (Larsen and Evans, 1978; Evans, 1979; Rzoska, 1980; Ya'acoub et al., 1981; Al-Azzawi, 1986; Sanlaville, 2002; Baltzer and Purser, 1990; Aqrawi, 2001). A marine unit of Holocene age (Hammar Formation) underneath the fluvial deposits was already detected by Hudson et al. (1957) in the Shatt-el Arab region. Hitherto, however, geological data are still lacking for the Lower Khuzestan plain. Therefore, the lateral extent of the Holocene marine deposits in the subsoil of the vast plain (ca. 28,000 km^2) is not adequately known. The only indication of marine deposits in Lower Khuzestan was reported by Thomas (quoted in Lees and Falcon, 1952, p. 34) who found marine and estuarine deposits north of Bandar Shahpur (now Bandar-e Imam Khomeini, Fig. 1). Also, the Holocene sea-level history and the timing and progress of the flooding of the Lower Khuzestan plain are poorly documented.

The study of palaeoenvironmental changes in the Lower Khuzestan plain is challenging, because of its rich archaeological heritage. One of the most ancient civilizations, the Elamite Kingdom (2700–539 BC) was primarily centred in the province of what is now called modern-day Khuzestan. Changes in coastal configuration could have had a profound effect on the population occupying the Khuzestan region from Elamite time to present. In this study, the Holocene sedimentary sequence of the Lower Khuzestan plain is investigated to reconstruct the Holocene evolution of the coastline and plain.

2. Study area

The Lower Khuzestan plain, located northwest of the Persian Gulf, forms the southeastern part of the

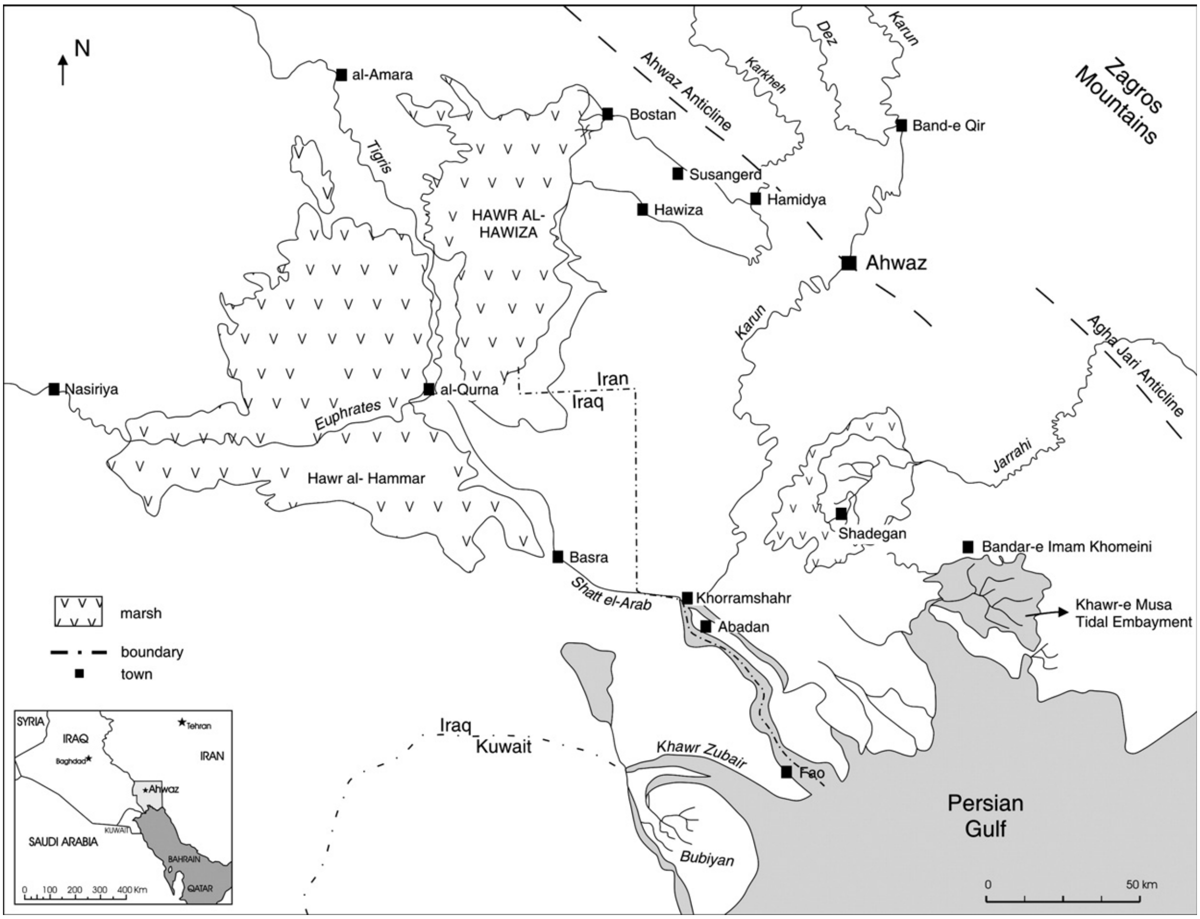

Fig. 1. Location map of the Lower Khuzestan plain (SW-Iran) along the northeastern extension of the Persian Gulf.

Mesopotamian foreland basin. The start of formation of the Mesopotamian foreland basin dates back to Plio–Pleistocene times (Zagros orogeny), when the Arabian and Eurasian plates collided (Haynes and McQuillan, 1974; Vita-Finzi, 1979; Audley-Charles et al., 1987). The plain is bordered to the north by the NW–SE oriented Ahwaz and Agha Jari anticlines of Miocene to Plio–Pleistocene age (James and Wynd, 1965; Setudehnia and O'B Perry, 1966; Macleod, 1969). The anticlines are crossed by the rivers Karkheh, Karun and Jarrahi, draining the relatively humid uplands of the Zagros mountains (Fig. 1). The river Karun crosses the Lower Khuzestan plain in a southwest direction and joins the Shatt-el Arab near the city of Khorramshahr. The river Karkheh flows into the Hawr al-Hawiza marshes located in the northwest of the plain. In the south, the Jarrahi river distributary fan system feeds the Shadegan marshes. The vegetation density (*Typha* and *Phragmites*) and extension of these marshes vary greatly, as a function of the seasonal rainfall regime.

The Lower Khuzestan coastline is today being shaped by a semi-diurnial mesotidal regime. The tidal range averages ca. 3–4 m along the coastline, increasing to 5–6 m in the Khawr-e Musa tidal embayment (Höpner, 1999; Admiralty Tide Tables, 2005; Fig. 1). At the city of Khurramshahr, located 50 km upstream on the Shatt-el Arab estuary, tidal amplitude averages ca. 1 m. Because of the gentle offshore slope (Purser, 1973), wave energy is very low. The tide-dominated coastline is fringed by a large tidal flat with a width up to 15 km, extending landward along the Khawr-e Musa tidal embayment. The vast intertidal area is bordered by supratidal salt marshes and clastic coastal sabkha's with saltpans. There is no freshwater inflow into the intertidal area, except in case of extreme river flood events.

3. Previous work

Since the early 19th century, historians and geomorphologists have debated the Holocene evolution of the Lower Mesopotamian plain, based on archaeological data, historical sources and surface observations. These early investigators were interested in the changes in the position of the Persian Gulf shoreline and the palaeocourses of the rivers Tigris, Euphrates and Karun as a result of the post-glacial sea-level rise. The earliest theories claimed that the head of the Gulf shifted far north of its present position, followed by a gradual retreat of the Gulf caused by delta progradation during prehistoric and historic ages. Beke (1835) placed the northern limits of the Persian Gulf inland of the Mesopotamian plain as far as Samara (100 km north of Baghdad). Ainsworth (1838) presented reports of a geological reconnaissance in southern Mesopotamia and suggested that the front of the delta had prograded over a distance of 112 km to its present position. De Morgan (1900) produced two maps (325 BC and 696 BC) based on accounts and reports from historical sources (cf. Baeteman et al., 2004/2005). The maps show the presumed position of the earlier coastline of the Persian Gulf between the cities Basra and al-Amara (Fig. 1).

Lees and Falcon (1952), on the contrary, challenged the 19th century concepts, and claimed that there was no evidence for the occurrence of an extensive marine flooding followed by delta progradation since the early Holocene. The authors suggested a delicately balanced system between subsidence (neotectonic effects) and sedimentation on occasion of local marine inundations. Nevertheless, they reported sediments containing marine and estuarine shells found in the subsoil of the plain as far inland as al-Amara (Iraq, Fig. 1). The same authors also invoked subsidence caused by neotectonics to explain the flooding of the Sassanian (220–640 AD) and Abbasid (758–1258 AD) irrigation canals nearby the present-day Khawr Zubair (Iraq) and Khawr-e Musa (Lower Khuzestan plain) tidal embayments (Fig. 1). The formation of the Khawr-e Musa tidal area was asserted to local subsidence and interpreted without further precision as being very young. Hudson et al. (1957) agreed with the views of Lees and Falcon (1952), contradicting their own identification of a landward extending Holocene marine unit (Hammar Formation) underlying the fluvial deposits of the Shatt-el Arab region.

The tectonic scenario as claimed by Lees and Falcon (1952) has been strongly criticised in the 1970s (Evans, 1979; Purser, 1973; Larsen, 1975; Larsen and Evans, 1978). These authors asserted that the Shatt-el Arab region has been more influenced by eustatic sea-level changes and deltaic progradation rather than by tectonic events. Macfadyen and Vita-Finzi (1978) suggested on the basis of faunal evidence and the presence of the Hammar Formation that a marine embayment extended as far inland as al-Amara (Iraq), followed by an overall delta progradation over a distance of about 150 to 180 km during the historical period. Later research carried out in the area also supported the view that Holocene sea-level changes controlled the evolution of the Shatt-el Arab region, rather than tectonics (Rzoska, 1980; Ya'acoub et al., 1981; Purser et al., 1982; Al-Zamel, 1983; Al-Azzawi, 1986; Sanlaville, 1989; Baltzer and Purser, 1990; Aqrawi, 1993; Aqrawi and Evans, 1994; Lambeck, 1996; Aqrawi, 2001; Sanlaville, 2002; Sanlaville and Dalongeville, 2005).

In literature, little is known about the post-glacial evolution of sea level in the Persian Gulf. According to the relative sea-level (RSL) curve of Dalongeville and Sanlaville (1987) it is assumed that sea level rose progressively in the Gulf basin from 14,000 yr BP onwards. RSL rise, as reconstructed by them, was particularly rapid between 9000 BP and 6000 BP and reached a maximum level of at least one or 2 m above present-day sea level at ca. 4300 cal yr BC, followed by a gradual sea-level fall to the present-day level, upon which some oscillations are superimposed. Dalongeville and Sanlaville (1987) identify four sea-level highstands (transgressions) during the period 6000–1000 cal yr BC and four sea-level lowstands (regressions) during 4500–200 cal yr BC. Moreover they suggest that the maximum amplitude of RSL change in the period 6000–1000 cal yr BC averages 2.5 to 3 m. The indicative meaning and age of the sea-level index points used by Dalongeville and Sanlaville (1987) for the reconstruction of the fluctuating RSL curve will be considered critically here, because the curve the authors published, seems generally accepted and frequently referred to. The sea-level index points are collected from three different regions along the Persian Gulf: Kuwait with the island of Failaka, Bahrein and Sharjah (United Arab Emirates). It is suggested that, despite the different regional contexts, the relative sea-level oscillations are contemporaneous for the three regions and that they are solely caused by eustatic changes. However, the authors admit that their data are not precise enough to affirm that these synchronic RSL changes were identical in the three regions. Moreover, the RSL indicators used by Dalongeville and Sanlaville (1987) are from various settings. They consider beach ridges that have been shifting horizontally with time; relict beach deposits above or below the present-day beach; submerged terrigenous and very shallow-water sediments; coastal settlements and/or occupation horizons and fixed biological sea-level indicators (coastal fauna). There is no exact information available about dated material, neither about their stratigraphical context. Possible contamination and height errors are also not discussed by Dalongeville and Sanlaville (1987). The accuracy of the use of relict beach deposits as sea-level indicator is difficult to estimate because raised beach deposits do not bear a well-defined relationship with mean sea level at the time of formation. Observations may systematically overestimate the highstand amplitude of mean sea level, as the correct level of storm surges is hard to infer from wave-dominated features and the reworking of shells remains uncertain. Other sea-level index points are on the basis of shell dating without taking into account the reservoir age of shells. The mid-littoral barnacle *Chatamales* and the sub-littoral species *Annelids* were used as fixed biological RSL indicators to identify a RSL highstand along the Island of Failaka and an RSL lowstand along the coastline of Bahrein, respectively (Dalongeville, 1990; Dalongeville and Sanlaville, 1987; Sanlaville et al, 1987). Fixed biological indicators are indeed reliable and sensitive as sea-level index point in most cases (Morhange et al., 1998), but the vertical range of their population limit must be considered critically. Dalongeville and Sanlaville (1987) and Sanlaville et al. (1987) also have not mentioned whether the measurements were obtained from one single vertical profile including both the fossil and its present equivalent. Oyster shells from a pit in the archaeological site of Yarmouq (Sharjah) located along a former shoreline, were also used to reconstruct the RSL curve (Dalongeville and Sanlaville, 1987). The authors assumed that humans did not carry their food far away from the coastline. But the age of the shells only dates the coastline, and does not provide any information on sea level.

Danlongeville et al. (1993), Sanlaville (1989, 2002) and Sanlaville and Dalongeville (2005) proposed a new general scheme for the evolution of Lower Mesopotamia on the basis of their previously published RSL curve. The authors produced three palaeogeographical maps showing the position of the Persian Gulf shoreline at ca. 4300 yr BC, during the Hellenistic period (323 BC) and the Medieval period (10th century AD), respectively. Evidence for a maximum post-glacial transgression at ca. 4300 BC in Lower Mesopotamia is recalled by Sanlaville (1989, 2002) and Sanlaville and Dalongeville (2005) from literature. They refer to radiocarbon dates of marine and estuarine deposits (Hammar Formation) found in the surrounding of Khor al-Hammar (Iraq) by Purser et al. (1982), Plaziat and Younis (1987) and Al-Azzawi (1986). The Hammar Formation was dated at 4310±160 BP (oysters) and 5020±90 BP on the southern shore of Lake Hammar; at 5730±210 BP north of Khor Abdallah, and at 4770±140 BP to the west of Lake Hammar. The authors suggest that these dates (around 5000 BP) correspond well with the period of maximum transgression identified by Gunatilaka (1986) in Kuwait. The latter identified five oolithic beach dune ridges in Kuwait, dated between 5500±70 BP and 2190±70 BP and suggested a sea-level maximum around 4630±60 BP. Sanlaville (1989, 2002) and Sanlaville and Dalongeville (2005) concluded that the presumed shoreline of the Persian Gulf at the post-glacial maximum (4300 BC) extended as far as the present-day villages of Nasirya (Iraq), Amara (Iraq) and Ahwaz (Iran, Lower Khuzestan, cf. Fig. 1). In Lower Khuzestan the present-day anticline of Ahwaz stopped the marine transgression. This implies, as suggested in Sumerian sources (Falkenstein, 1951; Jacobsen, 1960), that the third millennium (BC) cities of Ur and Eridu (Iraq) were located nearby the coastline. Sanlaville (1989, 2002) and Sanlaville and Dalongeville (2005) suggest that the post-maximum sea-level period is marked by a rapid progradation of the Tigris–Euphrates–Karun delta. However, the authors mention that they do not know when the Gulf reached its present shoreline. They suggest that during the Hellenistic period (323 BC) the coastline was located south of the present-day one, with a RSL at about 1 m below the present-day level as demonstrated in Bahrein and Failaka (Dalongeville, 1990). Based on the latter, Sanlaville and Dalongeville reject the map (325 BC) proposed by De Morgan (1900). Hansman (1978) already earlier contradicted De Morgan (1900) and considered that the southern limit of the Mesopotamian delta was very near to the present one during Hellenistic period. Moreover, Hansman (1978) claimed, using evidence from historical texts, that the Persian Gulf coastline has not changed appreciable since the Hellenistic Period. Sanlaville (2002), and Sanlaville and Dalongeville (2005) claim that since the Hellenistic period the coastline did not remain stable and they

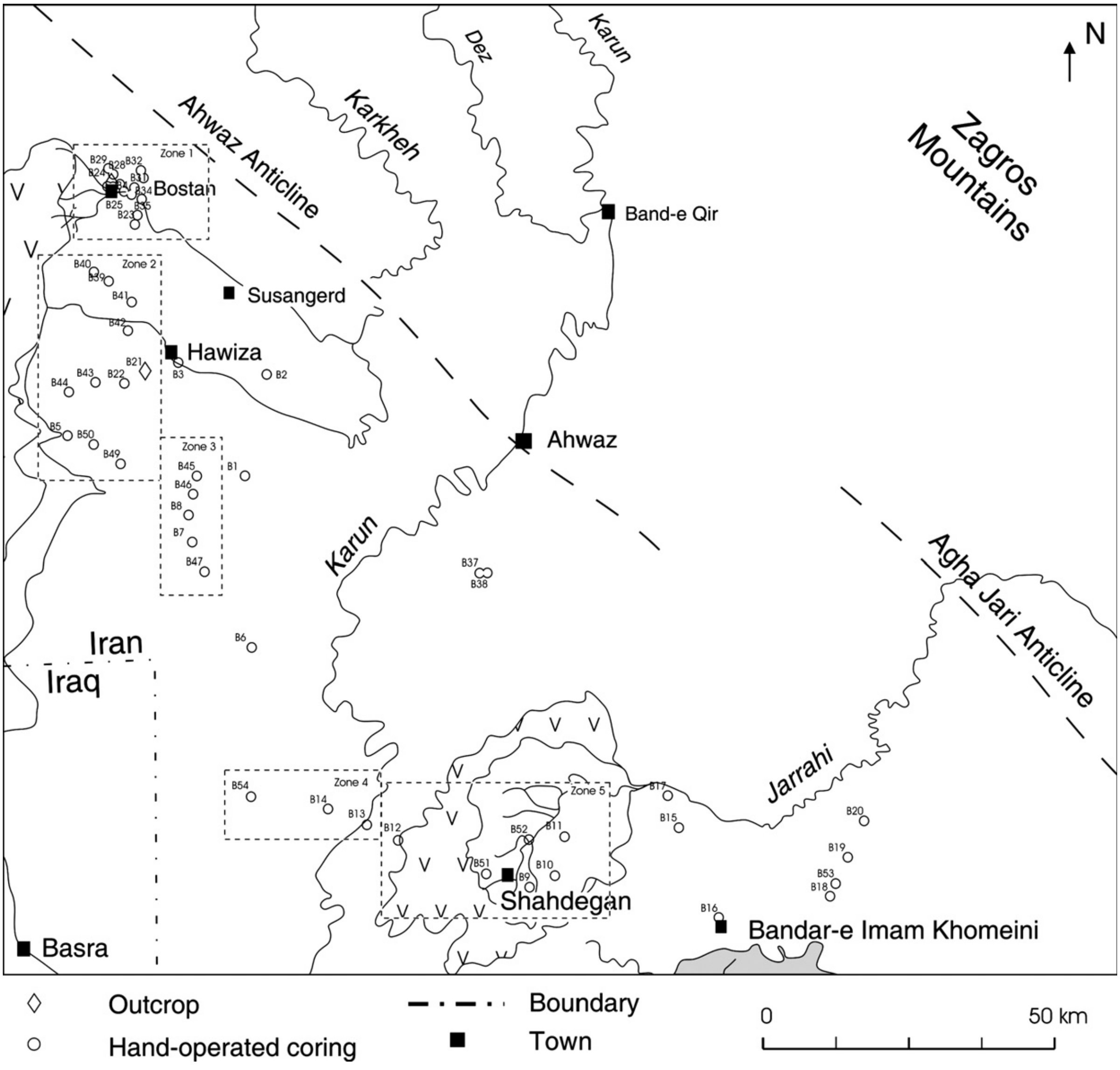

Fig. 2. Location map of the study area showing the location of core sites and outcrops. Zone 1: the active alluvial ridge of the Karkheh river; Zone 2: the area south of the active course of the Karkheh; Zone 3: the northern area west of the river Karun; Zone 4: the southern area the west of the river Karun; Zone 5: Jarrahi distributary system and brackish–freshwater marshes.

proposed a Medieval (10th century AD) RSL highstand, which implies an inland extension of the Gulf as far as the present-day village of Abadan (Fig. 1). Between Basra and Kufa, the authors draw an extensive marsh, that developed due to a rise of the groundwater table, related to a rise of RSL. The landward limit of the Gulf is based on the work by Le Strange (1905). Le Strange describes that the city of Abadan in the 11th century was located on an island in between the estuaries of the Karun and Tigris along the Persian Gulf coast. Le Strange (1905) also introduced the existence of 'The Great Swamp' located in between Basra and Kufa.

4. Methodology

For the stratigraphical investigation, 52 cores were collected manually and three shallow outcrops were surveyed and sampled during two field campaigns (Fig. 2). The coring was carried out using a gouge auger to obtain undisturbed and continuous cores to a depth of 5–10 m below the surface. A spiral auger was used to penetrate the compact clay layers. Borehole locations were registered using GPS. The surface elevation of the boreholes was inferred from topographic maps and site-specific measurements obtained at the regional topographic institute. In the field, the cores and outcrops were described on lithology, sedimentary structures and macrofossils and preliminary facies identification was made. Samples were taken for laboratory analyses when significant changes in color, texture or lithology were observed. A further interpretation of the different depositional (sub) environments was carried out on the basis of the integration of lithological and palaeoecological (foraminifera and diatom) analyses and is discussed in Heyvaert et al. (submitted of publication). Reconstruction of the spatial distribution of the different environments and their succession in time is based on cross-sectional lithological data in five different zones (Fig. 2).

Radiocarbon dates were obtained from organic material (Table 1) and shells and provide a chronological framework for the palaeogeographical reconstruction. Calibrated dates are given with a 2 sigma error range in

Table 1
AMS radiocarbon data and calibrated ages

Site	Geographical coordinates	Laboratory code	Age ^{14}C (yr BP)	Calibrated age (yr cal BP)	Sample altitude	Date material
B5	31°20′43″ 47°53′04″	KIA-24461	3270±30	3580–3390	+0.65	Organic gyttja
B6	31°01′11″ 48°12′31″	KIA-24465	1655±25	1510–1630	+3.95	Organic gyttja
B24	30°38′41″ 48°41′50″	KIA-24490	155±25	60–230	+**3.35**	Organic material
B24	30°38′41″ 48°41′50″	KIA-24480	250±25	270–320	+**2.50**	Peaty mud
B24	30°38′41″ 48°41′50″	KIA-24481	280±25	350–440	+**1.98**	Peaty mud
B26	31°43′10″ 47°58′53″	KIA-26488	80±30	20–150	+**3.55**	Peaty mud
B26	31°43′10″ 47°58′53″	KIA-26745	160±20	230–130	+**3.50**	Vegetation remnant
B34	31°41′50″ 48°01′45″	KIA-26474	95±20	20–140	+6.40	Vegetation remnant
B39	31°34′37″ 47°57′59″	KIA-26481	1350±25	1240–1310	+1.10	Organic gyttja
B44	31°24′43″ 47°53′18″	KIA-26719	7935±35	8980–8630	+0.90	Peaty mud
B49	31°18′07″ 47°58′45″	KIA-27131	450±25	483–530	+4.75	Peaty mud
B51	31°39′59″ 48°37′19″	KIA-26480	280±20	350–430	+2.75	Organic material
B54	30°47′44″ 48°12′00″	KIA-26482	6980±35	7710–7880	−3.70	Roots
B54	30°47′44″ 48°12′00″	KIA-26746	7275±35	8170–8010	−3.80	Fine roots
B54	30°47′44″ 48°12′00″	KIA-26747	7085±35	7980–7840	−5.40	Peaty mud

calendar years before present (cal BP). Calibration was completed using the calibration programme of Stuiver and Reimer (1993). Only bulk samples of organic sediments were used for age determination. These samples consist of organic material in a predominantly silty clayey matrix. Radiocarbon ages obtained from bulk samples may be affected by a number of potential error sources resulting in erroneously young or old ages (Mook and Steurman, 1983; Törnqvist et al., 1992). We are aware of this problem, however, because of the semi-arid climatic conditions, vegetation growth is restricted and the preservation of organic material is poor due to highly oxygenated conditions. Because the reservoir age of shells is not known yet the data are not reported here.

5. Results

5.1. Facies analyses and environmental interpretation

Sedimentary facies reflect the physical and chemical conditions of depositional environments. In the studied boreholes, three sedimentary units have been identified based on color, texture, macrofossil content, vegetation remnants and gypsum crystals and the stratigraphic position. Sediments belonging to these three units were interpreted as being deposited in a fluvial (Unit 1), coastal (Unit 2) and brackish–freshwater marsh (Unit 3) environment, respectively (Heyvaert et al., submitted for publication).

5.1.1. Unit 1

The sediments of Unit 1 consist of a very compact silty clay to clayey silt, reddish brown in color. The color and the stiffness of the clay are indicative of subaerial exposure (Baeteman, 1994). Rootlets, salt crystals and oxidation spots occur scattered and mollusc shells (*Corbicula* sp., *Melanoids* sp. and *Melanopsis* sp.) are abundant. In some cases, the unit is marked by the presence of more silty sand to sandy layers. The sediments of Unit 1 are interpreted as fluvial deposits comprising sandy to silty channel belt/crevasse-splay deposits as well as clayey to silty floodbasin deposits (Heyvaert and Weerts, submitted for publication).

5.1.2. Unit 2

Two sub-units have been differentiated: Units 2a and 2b.

5.1.2.1. Unit 2a. This unit looks at a first glance like a massive silty clay, in which an alternation of soft clay with more compacted silty clay layers can be observed. Burrowing structures are absent, and parallel lamination in the red-brown silty clay is well preserved. Towards the upper part of the unit, halite concentrations and gypsum crystals occur in the more compacted clay layers. Deformed and ruptured mm-laminae due to evaporite crystalisation are common in the upper part. Sediments of Unit 2a are interpreted as being deposited in the high intertidal to supratidal flat/clastic coastal sabkha environment. While aggrading to supratidal level, the red-brown laminated deposits experience more prolonged intervals of subaerial exposures between mean high and spring high-water levels. A clastic coastal sabkha sedimentary environment develops, in which gypsum crystals form in the upper intertidal area due to excessive evaporation during intervals of flooding and increasing upslope interstitial pore water salinity (Thompson, 1975; Saleh et al., 1999).

5.1.2.2. Unit 2b. Sediments of Unit 2b are characterised by a soft water-saturated soft clay (mud) or silty clay, blue to greyish in color, with brownish tints. The blue to greyish color is indicative of slightly reducing conditions. Vegetation remnants are sometimes present but bioturbation is completely absent. Unit 2b shows sometimes thin laminations of blue, brown-grey clay occurs. Laminae of silt and very fine sand alternate at irregular intervals of 1–3 cm within the laminated clay, gradually changing into a soft-water-saturated mud. According to the facies, it is suggested that deposits of Unit 2b represent a low-energy mud tidal flat. The laminations are interpreted as tidal bedding, formed in a subtidal and lower intertidal flat. The mud settled from suspension during periods of slack water and just before and after slack water conditions, while the interlaminated silt and very fine sand are deposited by tidal currents.

5.1.3. Unit 3

The sediments of unit 3 consist of a blue to greenish blue silty clay, with vegetation remnants and numerous molluscs (*Corbicula* sp., *Melanoids* sp. and *Melanopsis* sp.). The deposits show sometimes a crumbly structure, indicative of an initial physical ripening. The greenish color indicates the presence of pyrite. The iron is derived from detrital iron minerals, which are supplied by the rivers. In conjunction with simultaneously delivered organic material, reducing conditions are established within the sediment. Iron is released from the terrigeneous material and made available as easily soluble ferrous iron to form pyrite (Einsele, 1992). The sediments of Unit 3 are interpreted as being deposited in a brackish to freshwater marsh environment, possibly encompassing shallow-water bodies.

5.2. Cross-sections

5.2.1. The Karkheh Alluvial Ridge (Zone 1)

This zone is located in the northwest of the study area east of the Hawr al-Hawiza brackish–freshwater marshes and at about 200 km north of the Gulf. The areas on both sides of the active channel of the Karkheh were investigated with thirteen boreholes and one outcrop (Figs. 2, 3a and b).

Two boreholes were carried out outside the Holocene plain. B32 revealed dune deposits consisting of fine sand and sandy silt for 3 m, underlain by red-brown clay

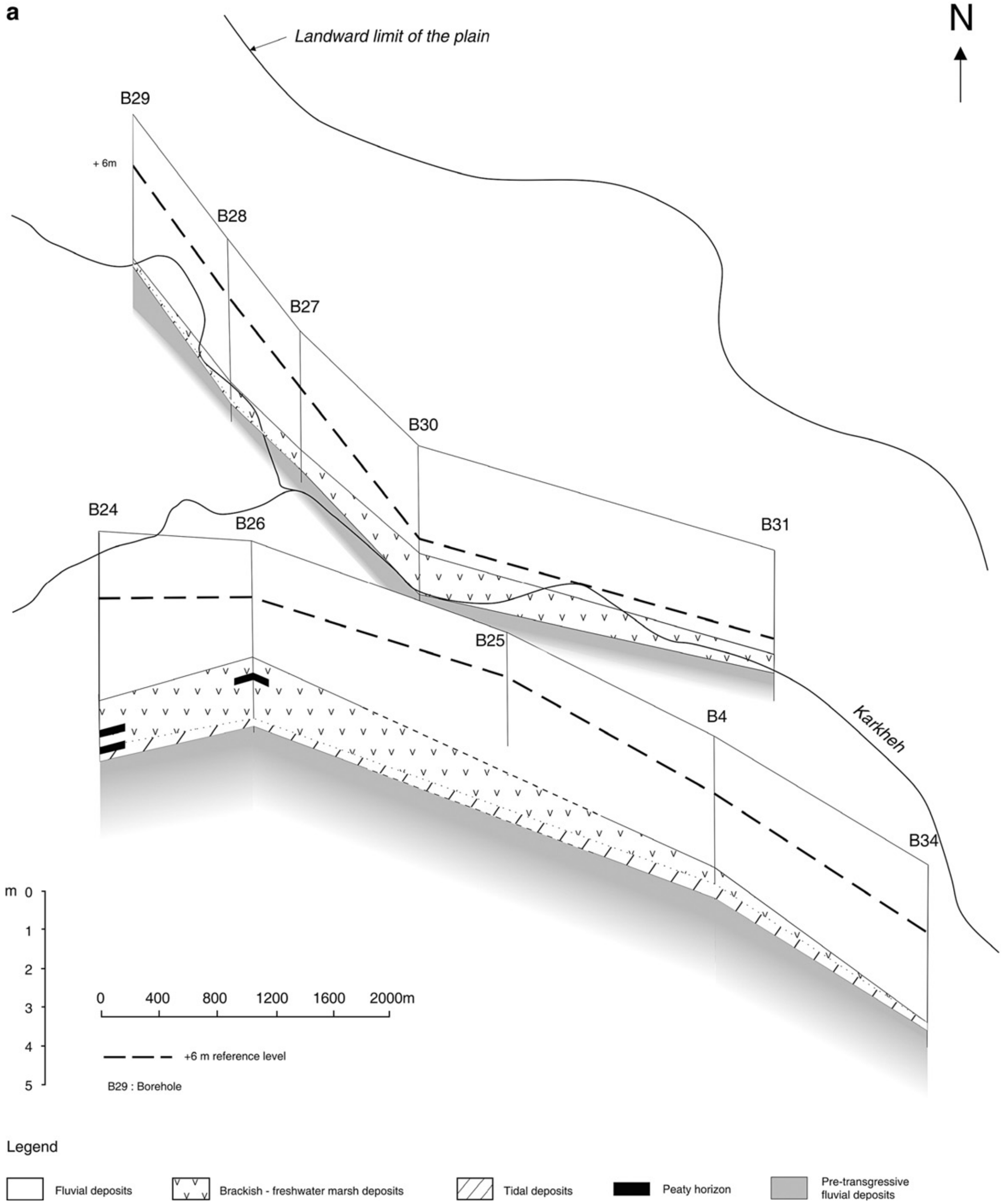

Fig. 3. a: Diagram with two stratigraphic sections that are located north and south of the active course of the river Karkheh, respectively (Zone 1). The delineation of the plain and the position of the cores are given in Fig. 3b.

Fig. 3. b: Map of the area along the active course of the river Karkheh, indicating the location of the stratigraphic sections (shown in Fig. 3a) and the delineation of the landward limit of the plain.

with small pebbles. No clay was recovered from B33. Here, the dune deposits are underlain by greenish brown clayey sand changing to sand, too hard to penetrate. The clay and sand are interpreted as belonging to the pre-transgressive Karkheh floodplain. The latter is limited in the north by the edge of the Ahwaz anticline. The dune deposits, covering the fluvial deposits, form the landward limit of the Holocene plain.

The borehole descriptions from this zone were brought together in a schematic diagram (Fig. 3a). The elevation of the pre-transgressive surface ranges between +2 and +5 m and is ca. 1 to 2 m higher north of the active course of the Karkheh than south of it. It is covered by tidal deposits gradually overlain by brackish–freshwater deposits widespread, thinning in an eastern and northwestern direction. These deposits reach an elevation ranging between +3.5 and +4 m, with a maximum at +5.5 m in B31. Only in core B24 and outcrop B26 peaty horizons were recovered. The upper part of the sedimentary succession in Zone 1 consists of fluvial deposits. In all of the boreholes, deposits of the pre-transgressive surface consist of red-brown clay covered by a thin layer of greenish brown sand. In B24, the pre-transgressive surface is overlain by an almost 2-m-

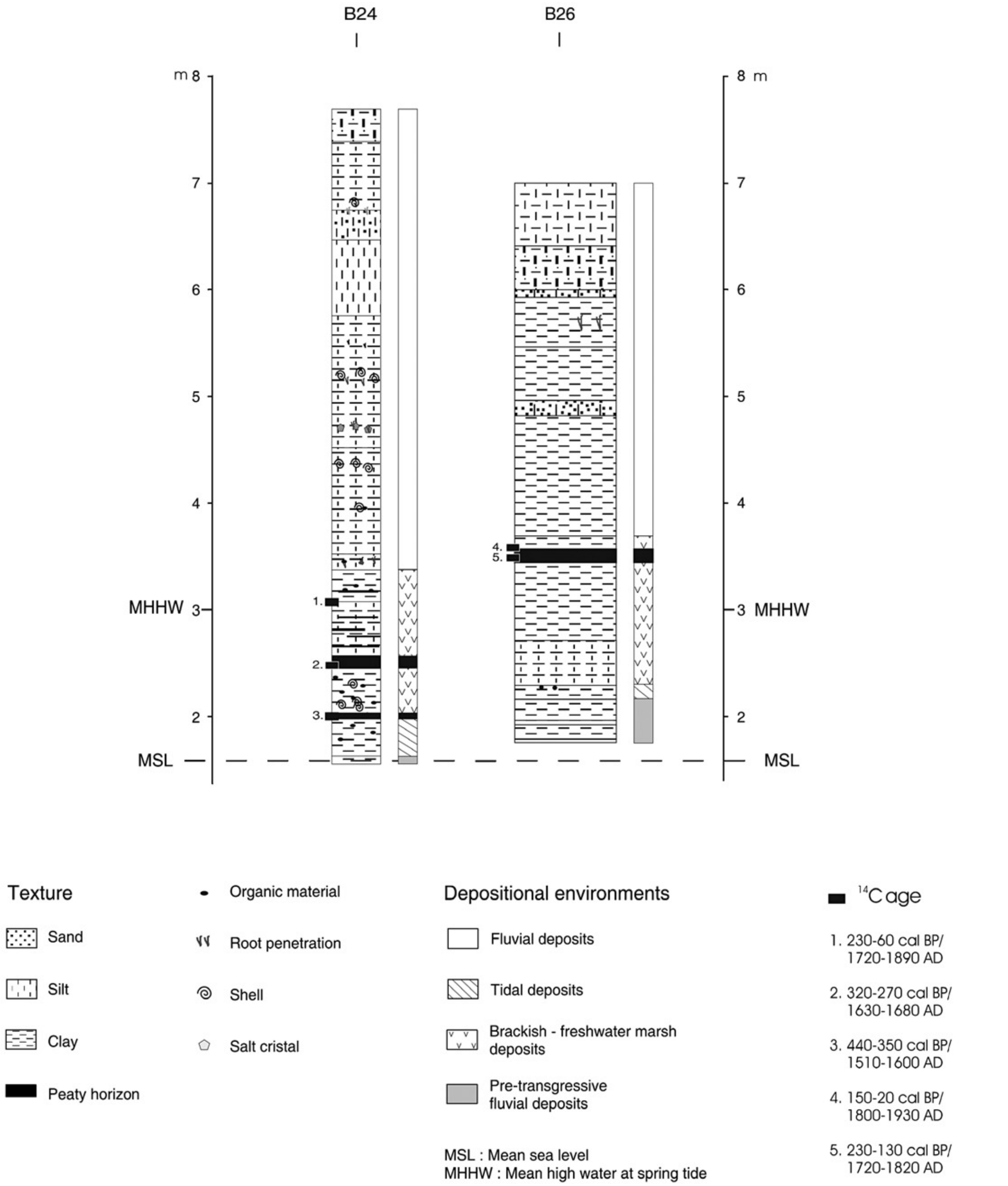

Fig. 4. Stratigraphy of core B24 and outcrop B26, located south of the active course of the river Karkheh (Zone 1), with indication of the depositional environments. The location of outcrop B26 and borehole B24 is given in Fig. 3b.

thick blue to greenish blue soft silty clay with two peaty horizons at a level of +1.98 and +2.50 m and abundant freshwater shells (*Corbicula* sp., *Melanoids* sp.) towards the top (Fig. 4). The peaty horizons have been dated at 350–440 cal BP and 270–320 cal BP, respectively (Table 1). Diatom analyses were undertaken of these two peaty horizons to complement the facies analyses (Heyvaert et al., submitted for publication). The peaty horizon at a level of +1.98 m bears an upper intertidal fauna with the indication of marine influence in the vicinity. At +2.50 m diatom fauna indicates a more brackish–freshwater environment. This suggests that the blue soft silty clay below +1.98 m was deposited in the upper reach of the intertidal zone. The peaty horizon at +1.98 m reflects a high intertidal brackish environment gradually changing to more brackish/freshwater marsh conditions. At +2.80 m, the peaty horizon is erosively overlain with a bluish grey to brown-grey silty soft clay showing oblique laminae. The brownish grey laminae are interpreted to contain reworked material and to represent a transition to even more freshwater conditions. Reworked organic material at the level of +3.35 m in B24 was dated at 230–60 cal BP. In outcrop B26, the base and the top of a peaty horizon, on a slightly higher level (+3.55 m) was dated at 230–130 cal BP and 150–20 cal BP. In all the boreholes the upper part of the sedimentary succession consists of a brown compact clay with few zones of brown silty soft clay, red-brown laminae, root penetrations, rootlets, and oxidation spots. These sediments are interpreted as being deposited by the present-day Karkheh fluvial system. The date of the peaty layer in B26, covered by the fluvial deposits, suggests that sedimentation by the river Karkheh started at the earliest at 150–20 cal BP. An additional date (20–140 cal BP) has been obtained from a vegetation remnant in the brown clay at an elevation of +6.5 m in B34. This age suggests the reworking of organic material. In view of the thickness of the fluvial deposits (ca. 3–4 m) and the short time span of deposition (max 150 yr), sedimentation rate was very high.

It is suggested that the region along the presently active channel of the river Karkheh was characterised by an upper intertidal environment evolving into a brackish–

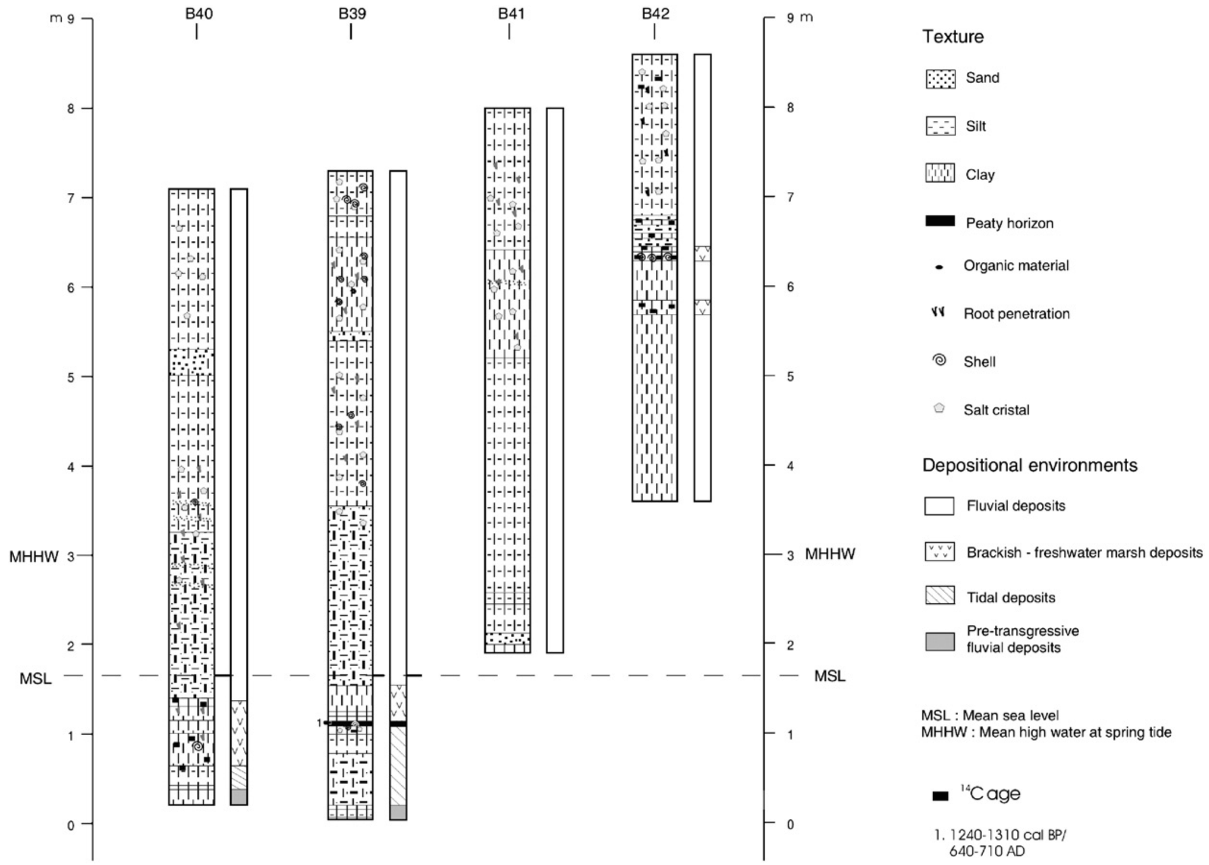

Fig. 5. Stratigraphic profile (with indication of depositional environments) of the cores located north of the abandoned course of the river Karkheh (Zone 2). The location of the boreholes is given in Fig. 2.

freshwater marsh environment, that after ca. 140 cal BP became filled with deposits of the river Karkheh. Most probably, the brackish–freshwater marsh environment formed a former eastern extension of the Hawr al-Hawiza marshes.

5.2.2. The area south of the active course of the Karkheh (Zone 2)

This area extends ca. 45 km south of the active course of the Karkheh and ca. 30 km west of Hawiza. It comprises the areas north and south of the abandoned Karkheh channel belt and borders the Hawr al-Hawiza marshes to the east (Fig. 2). Nine borings were carried out and two shallow outcrops were surveyed (Figs. 5–7).

A first series of boreholes is located north of the abandoned Karkheh channel (boreholes 39 trough 42, Fig. 5). Their elevation varies between +7 m and +8.5 m. The two cores in the very northwest (B39 and B40) show a similar sedimentary succession. The compacted red-brown clay at the base (at +0.25 m) has been interpreted as the pre-transgressive surface. In both cores it is overlain by a blue clay that is locally sandy at the base and from which an upward transition from intertidal *to* supratidal conditions can be inferred. In borehole B39 the latter is covered by a thin peaty mud or organic gyttja changing into a bluish to greenish blue soft clay with laminae of peat detritus and numerous mollusc shells (*Corbicula* sp., *Menalopsis* sp.). The soft clay is in turn erosionally overlain by a 30-cm-thick bluish grey clay. These bluish organic rich deposits are interpreted as being deposited in a brackish–freshwater marsh environment. The organic gyttja in B39 was dated at 1240–1310 cal BP. From a level of about +1.40 m, a 2m-thick grey brown fine sandy silt to sandy clay is found. From a level of about +3.5 m, the sedimentary succession of B39 and B40 consists of a homogeneous rather of a compact greyish brown silty clay and brownish grey clay with salt crystals, freshwater shell fragments, root penetrations and vegetation remnants scattered all over. The latter is interpreted as floodbasin deposit of the abandoned palaeochannel of the river Karkheh. The sandy silt to sandy clay deposit from a level of +1.40 m is interpreted as channel belt/crevasse-splay deposits (Heyvaert and Weerts, submitted for publication). The sedimentary succession in core B39 and B40 suggests a gradual inundation of the pre-transgressive surface with brackish tidal influence, evolving from ca. 1240–1310 cal BP into a brackish–freshwater environment with the development of a dense vegetation. This resulted in the accumulation of organic material for a certain period. The erosional boundary

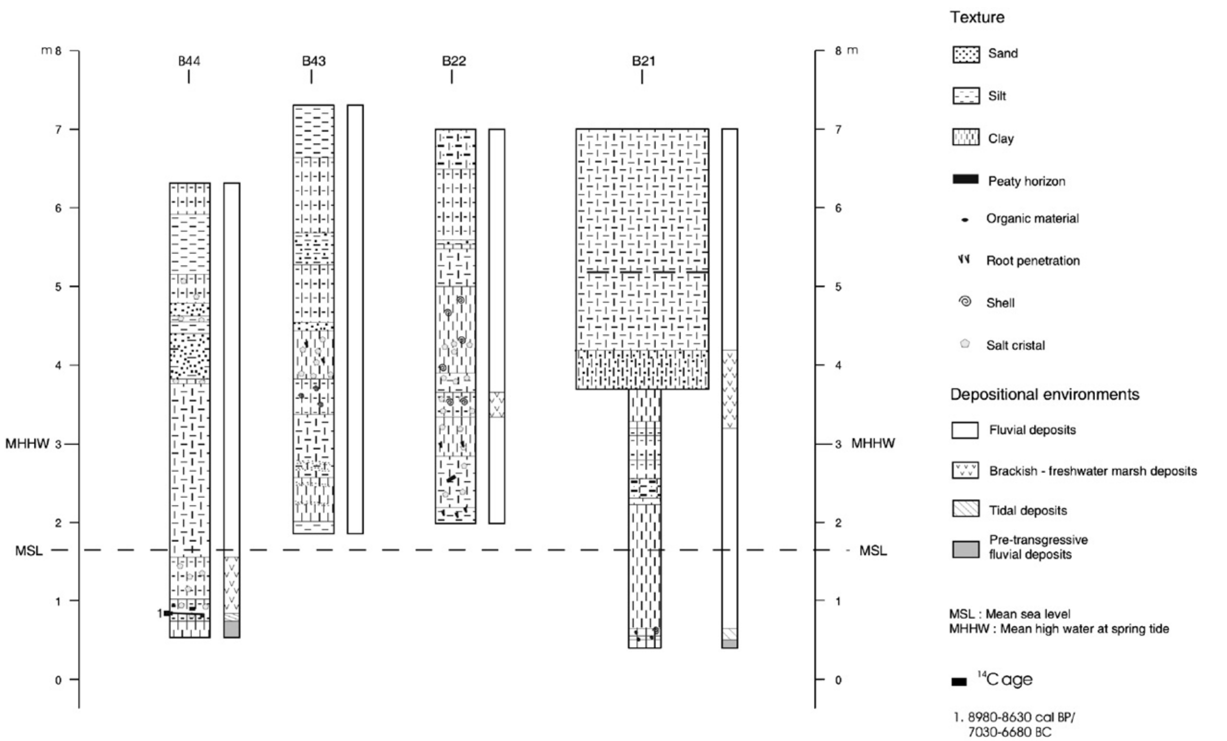

Fig. 6. Stratigraphic profile (with indication of depositional environments) of the cores and outcrop located south of the abandoned course of the Karkheh (Zone 2). The location of the boreholes and outcrop is given in Fig. 2.

present in B39, together with the laminae of peat detritus, indicates that the top of the peaty mud has been eroded by fluvial activity of the Karkheh. Fluvial sedimentation started at least after 1240–1310 cal BP (Heyvaert and Weerts, submitted for publication). The brackish–freshwater marsh deposits, which underlie the fluvial deposits, can be attributed to a former extension of the Hawr al-Hawiza marshes. In boreholes B41 and B42 no coastal deposits were found. Unfortunately, it was impossible to penetrate the compact clay of fluvial origin and it is not known whether the coastal deposits are present at greater depth. In B42, situated at a closer distance to the palaeochannel of the Karkheh, marsh deposits rich in freshwater shells and black vegetation remnants, were encountered at a level of +5.75 m and +6.20 m, respectively.

A second series of boreholes (B44, B43, B22; Fig. 6) and one outcrop (B21) are located more to the south. Their elevation ranges between +6 m and +7 m. In none of the boreholes the groundwater level was reached during coring. Nearby B44, B43 and B22 numerous shells (*a.o. Corbicula*) were found at the surface. Most probably these shells originate from a former extension of the Hawr al-Hawiza marshes, which are mainly fed by the rivers Tigris and Karkheh. In boreholes B43 and B22 no intertidal deposits were found. B44 and B21 reached deep enough to encounter the blue soft clay covering the compact clay at +0.70 m. The latter is also interpreted here as the pre-transgressive surface. In B44 the soft clay is overlain by a thin slightly peaty soft clay, which in turn is overlain by a greenish blue silty soft clay rich in salt crystals. The peaty soft clay occurs in the same stratigraphical position as in B39, but slightly deeper. Therefore it is assumed that its age should be ca. 1300 cal BP. However, it has been dated at 8980–8630 cal BP, suggesting that it contains old reworked material. The greenish blue silty clay overlying the peaty horizon is interpreted as being deposited in a brackish–freshwater marsh environment. Borehole B22 and outcrop B21, which are located more to the east,

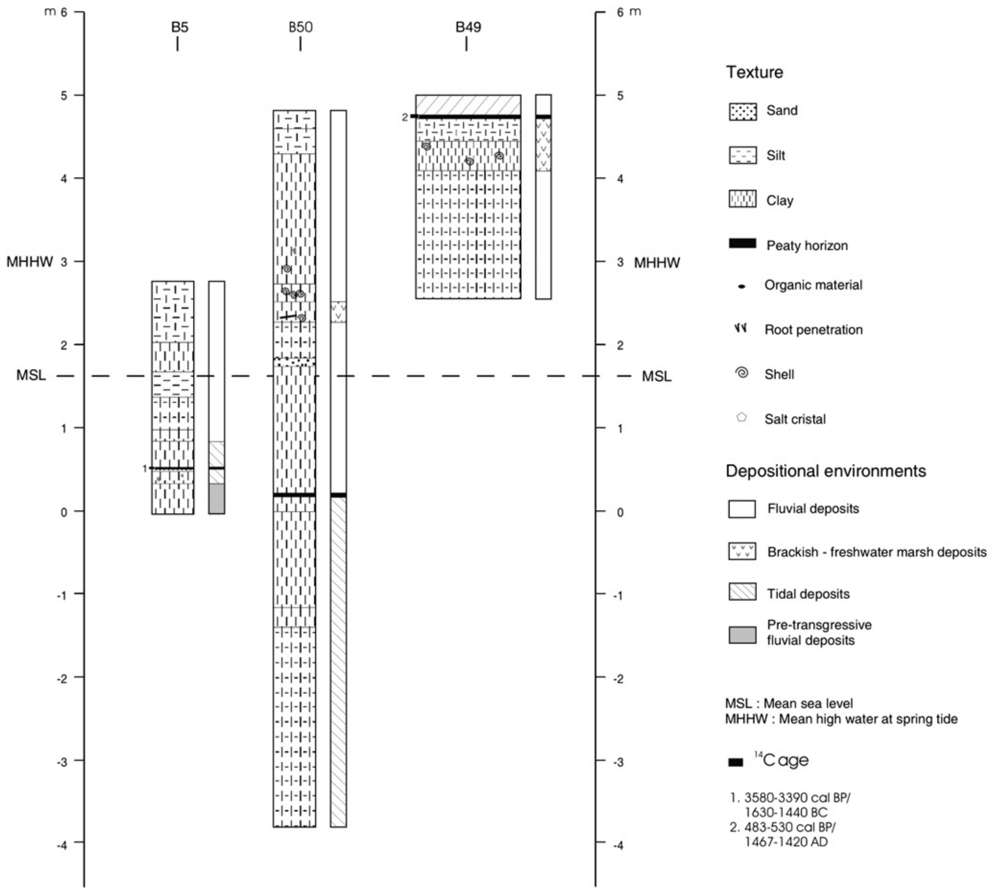

Fig. 7. Stratigraphic profile (with indication of depositional environments) of the cores and the outcrop in the area south of the abandoned course of the river Karkheh (Zone 2). The location of the boreholes and outcrop is given in Fig. 2.

show an intercalation of brackish–freshwater marsh deposits between +3 and +4 m in the brown silty clay of fluvial origin.

Of the southernmost series of boreholes (B5 and B50) and shallow outcrop B49 (Fig. 7), only B50 reached deep enough to recover coastal deposits. The elevation of the plain here is between +3 m and +5 m. The sedimentary succession in B50, starting at a level of −3.85 m, consists of interlayered clay and fine sandy silt, gradually changing into soft clay. It is interpreted as being deposited in the sub- and/or intertidal zone. It is covered by a 20-cm-thick layer of greenish soft clay with a thin layer of organic gyttja on top of it (at approximately 0 m). This represents a vertical shift from the intertidal to the supratidal zone, which eventually evolved into a marsh environment. It is overlain by a 4-m-thick red-brown clay in which a 25-cm-thick greenish grey clay with organic material of a brackish–freshwater marsh is intercalated at a level of +2.3 m. Also in B49, located more to the east, brackish–freshwater marsh deposits were found, but at a much higher level (+3.75 and +4.75 m). The presence of a peaty horizon at +4.70 m, dated at 483–530 cal BP, suggests that marshes could prevail for a time sufficiently long for peat accumulation. It implies also that the groundwater table was sufficiently high and that the vegetation did not suffer from excessive evapotranspiration. Most probably these brackish–freshwater marsh deposits are related to a former extension of the Hawr al-Hawiza marshes. The upper part of B5 (Fig. 7) shows a somewhat different sediment succession. At +0.7 m, the pre-transgressive surface is overlain by a greenish soft clay with root penetrations. It is covered by a thin white calcareous mud capped by an organic gyttja. A 20-cm-thick blue soft clay showing laminae of organic material forms the top of this particular interval, which is then overlain by a brown and red-brown clay. The organic gyttja was dated at ca. 3390–3580 cal BP. This interval most probably shows a vertical succession whereby the pre-transgressive surface became flooded forming a shallow pond in which the calcareous mud and organic gyttja accumulated. It indicates a rise in the groundwater level, most probably as precursor of the increase in tidal influence, which filled the pond at this particular site. The difference in stratigraphy between B5 and B50 can be explained due to the existence of a depression in the morphology of the pre-transgressive surface at B50. This depression was first filled subtidally, and this occurred before 3500 cal BP.

5.2.3. The northernmost area west of the Karun (Zone 3)

This zone is the northernmost investigated area west of the Karun. It is located at about 30 km to the east of the present-day Hawr al-Hawiza marshes. The elevation of the plain ranges between +5 and +7 m. Five borings were carried out in a north–south transect (Fig. 8). Only B46 and B47 reached deep enough to recover coastal deposits. The lower part of boreholes B7 and B45 consist of at least 1.5-m-thick brownish grey silty sand to brownish green sand gradually covered by sandy silt, interpreted as channel-belt/crevasse-splay deposits. The lower part of the sedimentary succession in B46 shows a ca. 3-m-thick (−3.5/−0.5 m) greyish clay with subtle laminations of silt, gradually changing into a soft clay. This 3-m-thick sequence was deposited in the intertidal zone. It is covered by a 20-cm-thick bluish green soft clay, which is in turn covered by a 2-m-thick red-brown clay. No gypsum crystals or vegetation remnants were found in this brown clay. Therefore it is not known whether it reflects the continuation of deposition in a supratidal environment, or whether it consists of fluvial sediments. However, the presence of the 1.5-m-thick channel-belt/crevasse-splay deposit in the lower part of boreholes B45 and B7, suggests fluvial deposition. The lower part of core B47 is characterised by the presence of greenish blue clay with brown spots covered at −2 m by a 1.5 m-thick-package of red-brown clay. It is overlain by a 20-cm-thick layer of bluish green silty soft clay with black organic spots, oxidation spots and gypsum crystals. The sedimentary succession of borehole B47 indicates deposition at high intertidal to supratidal level, occasionally flooded. The groundwater table, however, was not sufficiently high, or fluvial sediment input was too high for organic material to accumulate. Indeed, similar to borehole B46, the high intertidal to supratidal deposits are overlain at a level of ca. −0.5 m by a 2-m-thick red-brown homogeneous clay, which is covered by a 4-m-thick-package of compact brownish clay that is rich in root penetrations, salt crystals and black organic spots. Both brown to red-brown clay deposits are interpreted as being of fluvial origin.

The sedimentary succession of Zone 3 shows a gradual transition from brackish to freshwater conditions. Heyvaert and Weerts (submitted for publication) suggest that the channel-belt/crevasse-splay deposits found at the base of B45 and B7 can be associated to a palaeochannel belt of the river Karun. This palaeochannel belt was active until the latest 1240 cal BP. The time of onset of sedimentation by this palaeochannel belt could not be estimated, but started at least after 2300 cal BP.

5.2.4. The southernmost area west of the Karun (Zone 4)

This zone is the southernmost investigated area west of the Karun (Fig. 2). It is located at about 40 km north of the Shatt-el Arab. The elevation of the plain ranges between +3 m and +4 m. Numerous *Corbicula* shells are scattered all over the surface in the westernmost area. Three borings B54, B14 and B13 were carried out in a 30-km-long transect oriented perpendicular to the present-day Karun. Boreholes B14 and B13 are located at a distance of respectively 10 and 1.3 km to the west of the Karun.

The westernmost borehole, B54, revealed a compact red-brown clay at −5.50 m (Fig. 9). It is overlain by a thin blue soft clay containing numerous reed fragments, dated at 7980–7840 cal BP, followed by about a 1-m-thick grey silty soft clay with large bladed gypsum crystals, and a 1-m-thick blue silty soft clay with many vegetation remnants. At −3.70 m and −3.60 m, respectively, a vegetation horizon was found. The upper one was dated at 7880–7710 cal BP and the lower one at 8170–8010 cal BP. Between −3 m and −2 m, the sediments become more and more sandy upward showing a clear tidal bedding of fine sand, silt and soft clay. From −2 m upwards, the sand content in the soft clay diminishes rapidly and the 3.5-m-thick package of overlying sediments consist of brown clay alternating with soft clay. Numerous gypsum crystals are scattered all over. The uppermost part of the sedimentary succession shows brown and red-brown clay with oxidation spots indicating deposition above the groundwater table.

The sedimentary sequence in B54 can be interpreted as follows. The blue soft clay at the base indicates the start of the inundation of the pre-transgressive surface as a result of the post-glacial sea-level rise at or shortly before 8000 cal BP. The vegetation horizons indicate that a salt marsh with reed growth developed, however, not for a time sufficiently long for peat to accumulate indicating that the RSL rise was still rapid and sediment supply was too large. The marsh changed into an intertidal mudflat frequently silting up to supratidal levels. In view of the large bladed gypsum crystals in the lower part, the supratidal environment first developed into a salt flat or clastic coastal sabkha. Between ca. 7700 and 8200 cal BP, the sabkha changed into a high intertidal

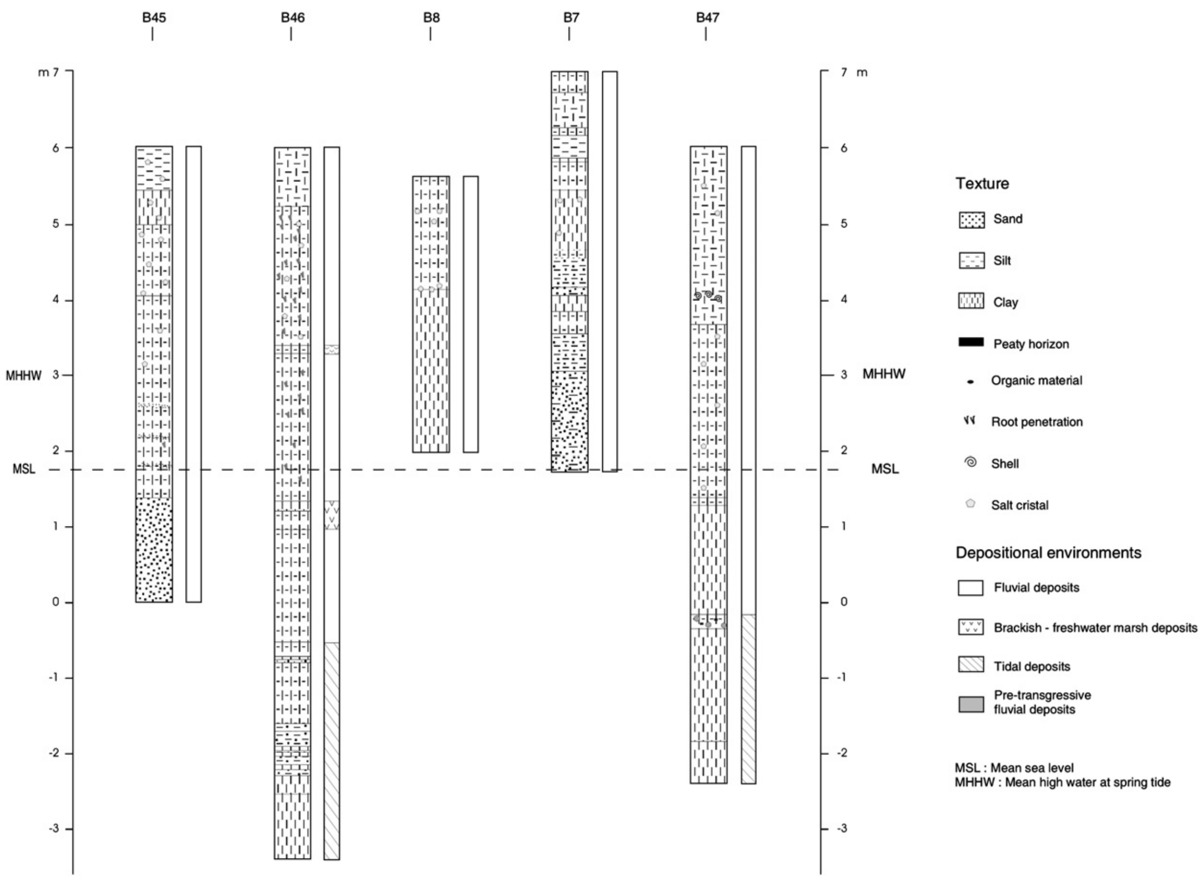

Fig. 8. Stratigraphic profile (with indication of depositional environments) of the cores located in the northern area west of the Karun (Zone 3). The location of the boreholes is given in Fig. 2.

area frequently silting up into a salt marsh with a dense vegetation cover. This vertical succession is to be explained by a lateral landward shift of the tidal environment as a result of the RSL rise forcing the coastline to migrate landward. Eventually, the area became completely within the sub- and intertidal reach. Later, the area started to silt up and changed again into a high intertidal and supratidal environment frequently evolving into a sabkha, represented by the package between −2 and +1.75 m. This change reflects the end of the landward shift of the tidal environment and coastline, and the start of the progradation of the coast. It also reflects that the impact of the RSL rise diminished. However, there is no time indication for this change. In view of the considerable sediment aggradation (3.5 m), the high intertidal and supratidal environments must have prevailed here for quite a long time. The very end of the sedimentary sequence (above +2.5 m) represents the replacement of the supratidal environment by floodplain.

In B14, located closer to the Karun, only the upper part, which was found in B54, was recovered. At +1 m in B14, a 40-cm-thick greenish grey soft clay with organic laminae and juvenile *Corbicula*, interpreted as marsh deposits, overlays tidal deposits. It indicates that here the supratidal environment already changed into a brackish–freshwater marsh, while in B54 at the same level, the supratidal flats prevailed. The upper part of B14 consists of brown silty clay and is interpreted as fluvial. The

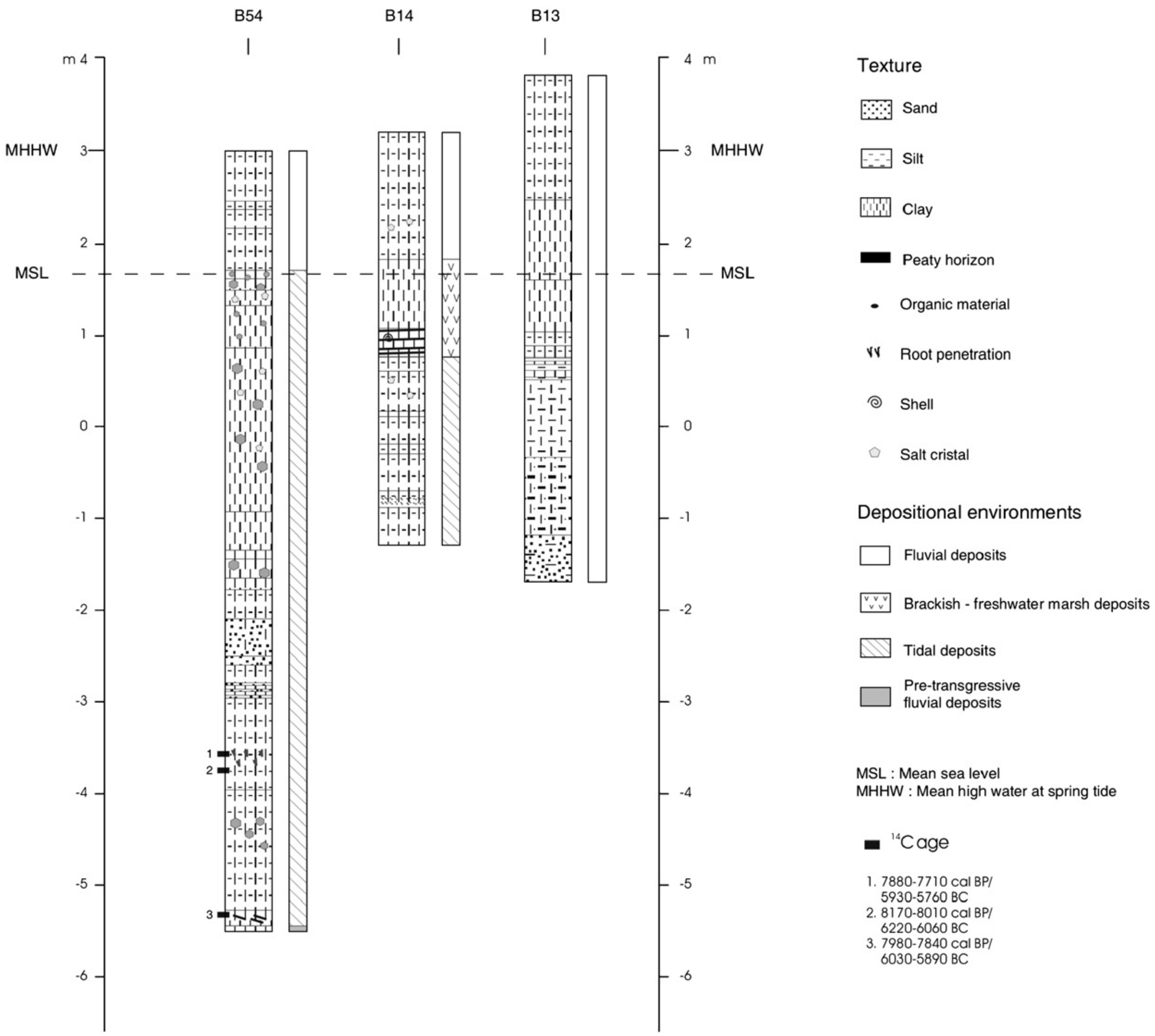

Fig. 9. Stratigraphic profile (with indication of depositional environments), of the cores located in the southern area west of the Karun (Zone 4). The location of the boreholes is given in Fig. 2.

lower part of B13 consists of greyish brown sand to silty sand gradually covered by brownish grey silty clay and sandy silt with intercalated layers (10–30 cm) of red-brown greyish mottled compact clay. These deposits are interpreted as channel-belt/crevasse-splay deposits of the Karun. Also the upper part of the sedimentary

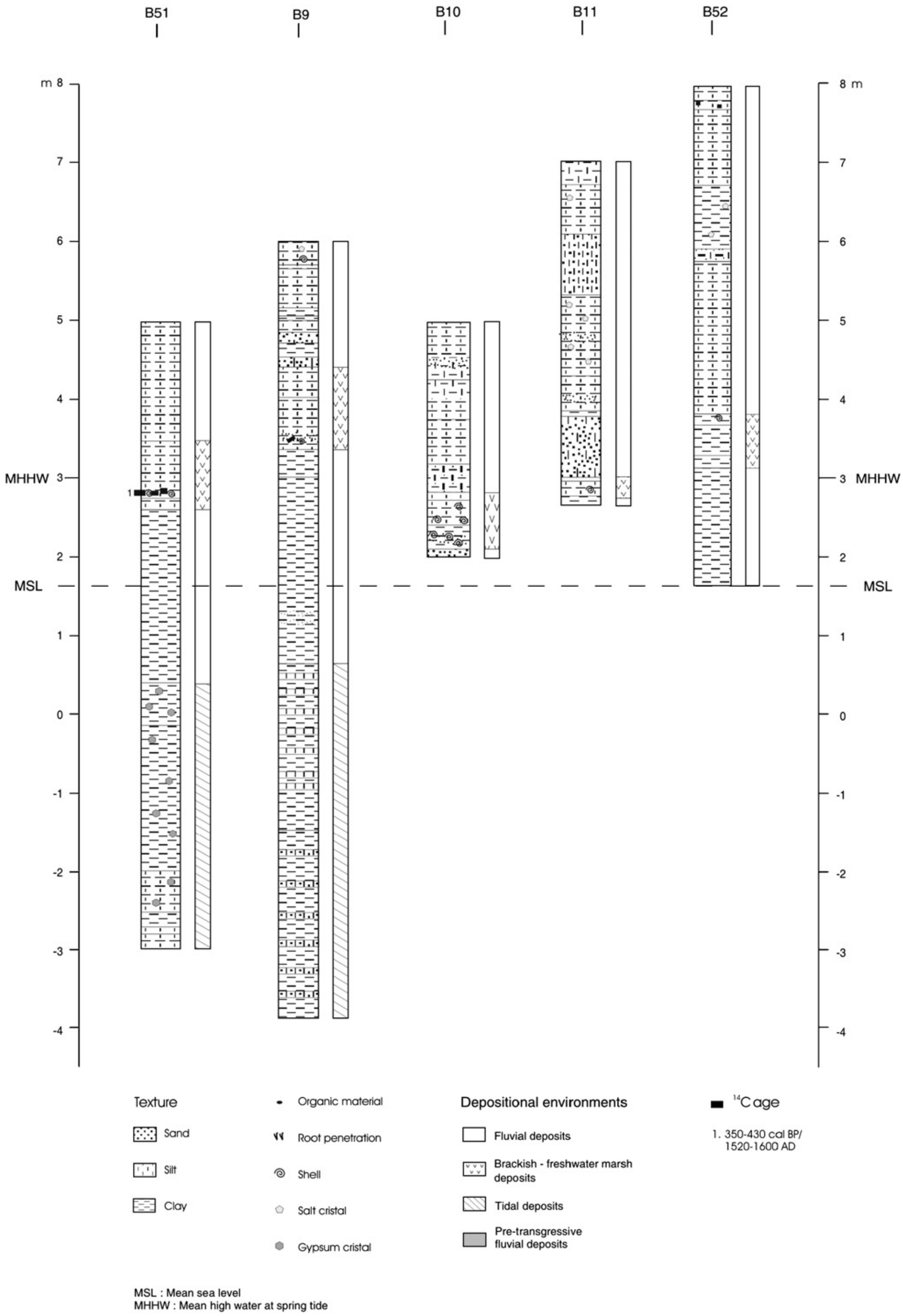

Fig. 10. Stratigraphic profile (with indication of depositional environments) of the cores located in the Jarrahi alluvial distributary system (Zone 5). The location of the boreholes is given in Fig. 2.

succession in B13 is interpreted as fluvial. Comparing B13 with B14 and B54, it seems that the river Karun has eroded vertically into underlying supratidal deposits (Heyvaert and Weerts, submitted for publication).

The sedimentary succession of Zone 4 clearly shows the progressive infill of a tidal embayment along the Shatt-el Arab, which at this location, most probably started before ca. 8000 cal BP. This indicates that the lateral extension of the Persian Gulf reached at least as far as 80 km north of its present position. Once the impact of the RSL rise became less important, most probably due to a reduced rate of RSL rise, the coast started to prograde, leaving behind successively coastal sabkhas and salt marshes. Progradation seems to be controlled to a great extent by fluvial sediment input by the Karun. Heyvaert and Weerts (submitted for publication) suggest that the Karun shifted to its present-day position by 1240–1000 cal BP and incised into underlying tidal deposits.

5.2.5. The Jarrahi distributary system and the Shahdegan freshwater marshes (Zone 5)

This zone is the southernmost investigated area of the Lower Khuzestan plain, close to the present-day Khawr Musa tidal embayment (Fig. 2). The zone consists of the Jarrahi distributary system and its surrounding brackish–freshwater marshes. The elevation of the plain ranges between +5 and +8 m. Five boreholes were carried out; only two of them, B9 and B51 (Fig. 10), penetrated the compact clay and were deep enough to recover coastal deposits.

The lower part of the sedimentary succession in B9 shows a ca. 2-m-thick (−3.70/−1.50 m) dark bluish grey deposit in which 1-to-5-cm-thick oblique laminae of fine sandy silt and silty soft clay alternate. This part displays the typical facies of a tidal bedding. It is overlain by a package of brownish grey silty soft clay, subtly laminated with silt, reaching to a level of +0.75 m. Between +0.75 m and +3.5 m, the sedimentary succession consists of a

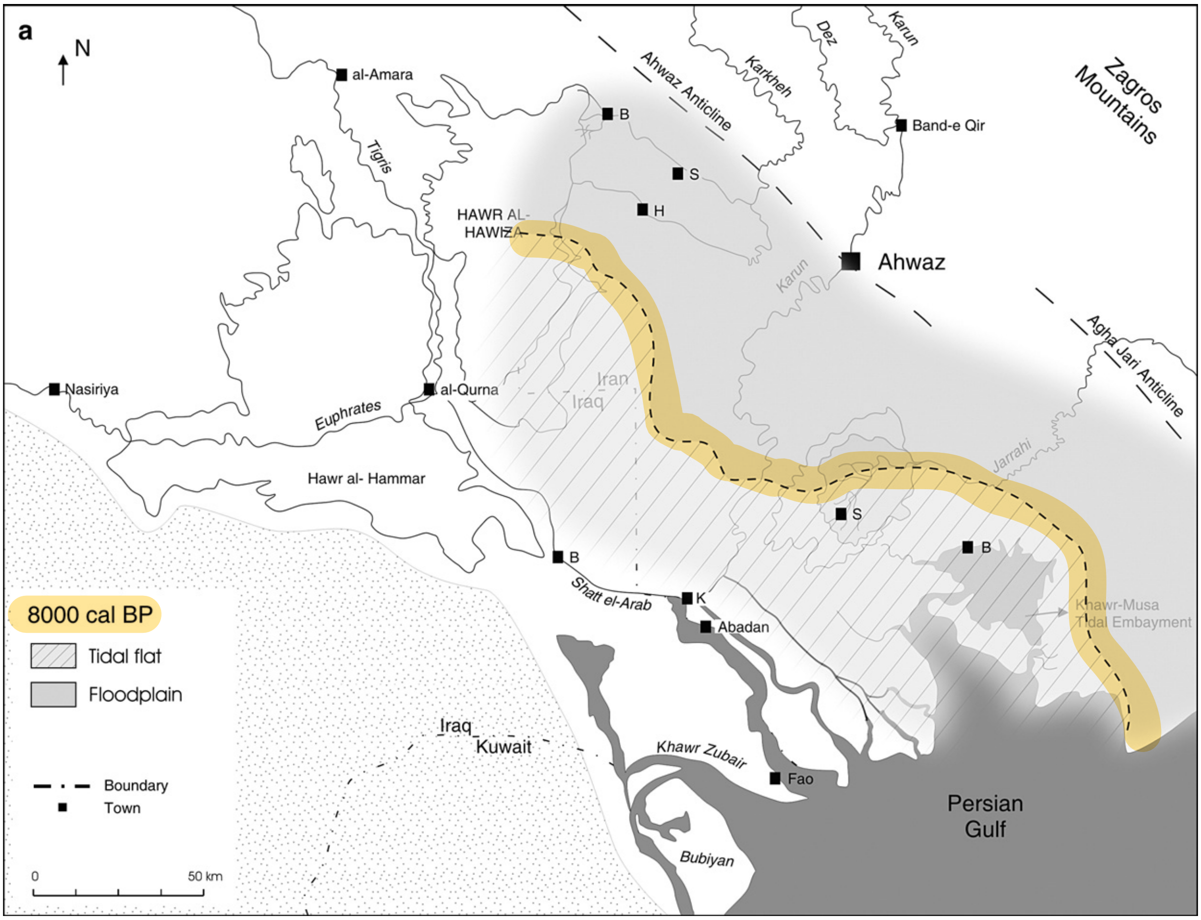

Fig. 11. Reconstruction of the environmental setting of the Lower Khuzestan plain around 8000 cal BP.

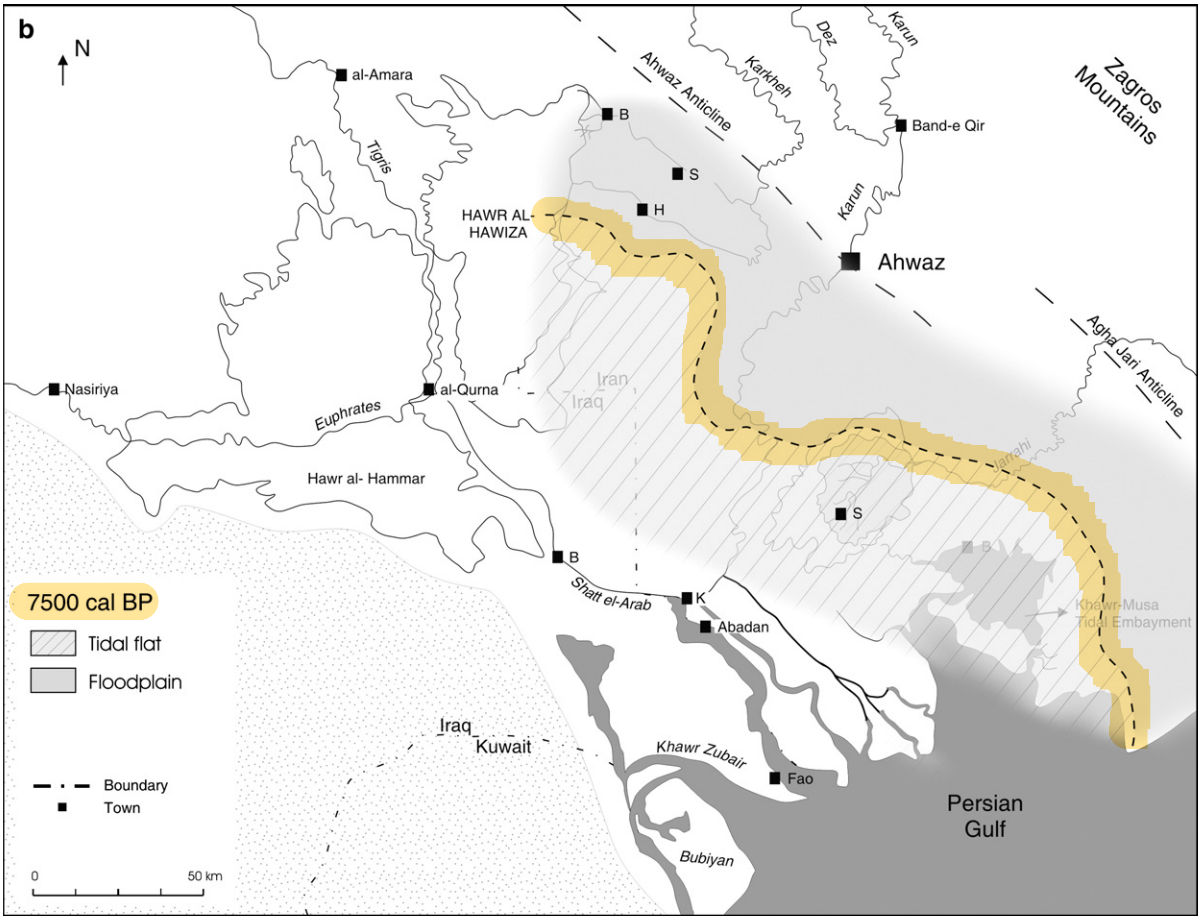

Fig. 11. Reconstruction of the environmental setting of the Lower Khuzestan plain around 7500 cal BP.

homogeneous grey brown clay, interpreted as fluvial. It is covered by a greenish blue silty clay with vegetation remnants and freshwater shells, deposited in a brackish–freshwater marsh environment. The brackish–freshwater marsh deposits are overlain by a grey brow clay of fluvial origin, in which oxidation spots and red-brown sandy and crumbly zones occur, as well as zones with soft clay.

B51 (Fig. 10), located at the boundary between the Shahdegan marshes and the Jarrahi distributary system, does not display the subtidal deposits at its base. The lower part of this core (−3.0 to −2.5 m) consists of dark blue soft clay with subtle laminations of silt indicative of intertidal deposition. Between −2.5 and +0.5 m, it is covered by brown soft clay containing gypsum crystals. Similar to borehole B9, the upper part of the sedimentary succession of B51 is characterised by a homogeneous brown compact clay (+0.5 to +2.75 m) covered by brackish–freshwater deposits between +2.75 m and +3.5 m. The brackish–freshwater-marsh deposit is at a slightly lower level than in B9. An organic horizon in its lower part was dated at 350–430 cal BP. The upper sediments of borehole B51 consist of a brown and red-brown silty clay with sandy zones, deposited by the Jarrahi distributary system. Boreholes B10, B11 and B52, showing only the upper part of the sedimentary sequence, also reveal the presence of brackish–freshwater marsh deposits intercalated in fluvial deposits.

The sedimentary succession of Zone 5 clearly shows the gradual infill of a tidal embayment. Borehole B9 displays a silting-up succession of tidal deposits. The base of it, however, was not recovered. The lower part in the core is deposited subtidally with a gradual upward change to intertidal deposition. This locality possibly reflects the silting up of a tidal channel. It is suggested that the impact of the RSL rise decreased, together with a seaward shift of the tidal environment. This regressive tendency is also reflected in the sedimentary succession of core B51, marked by sabkha deposits rich in bladed gypsum crystals. The upper part of the sedimentary sequence reflects that fluvial sediment supply became

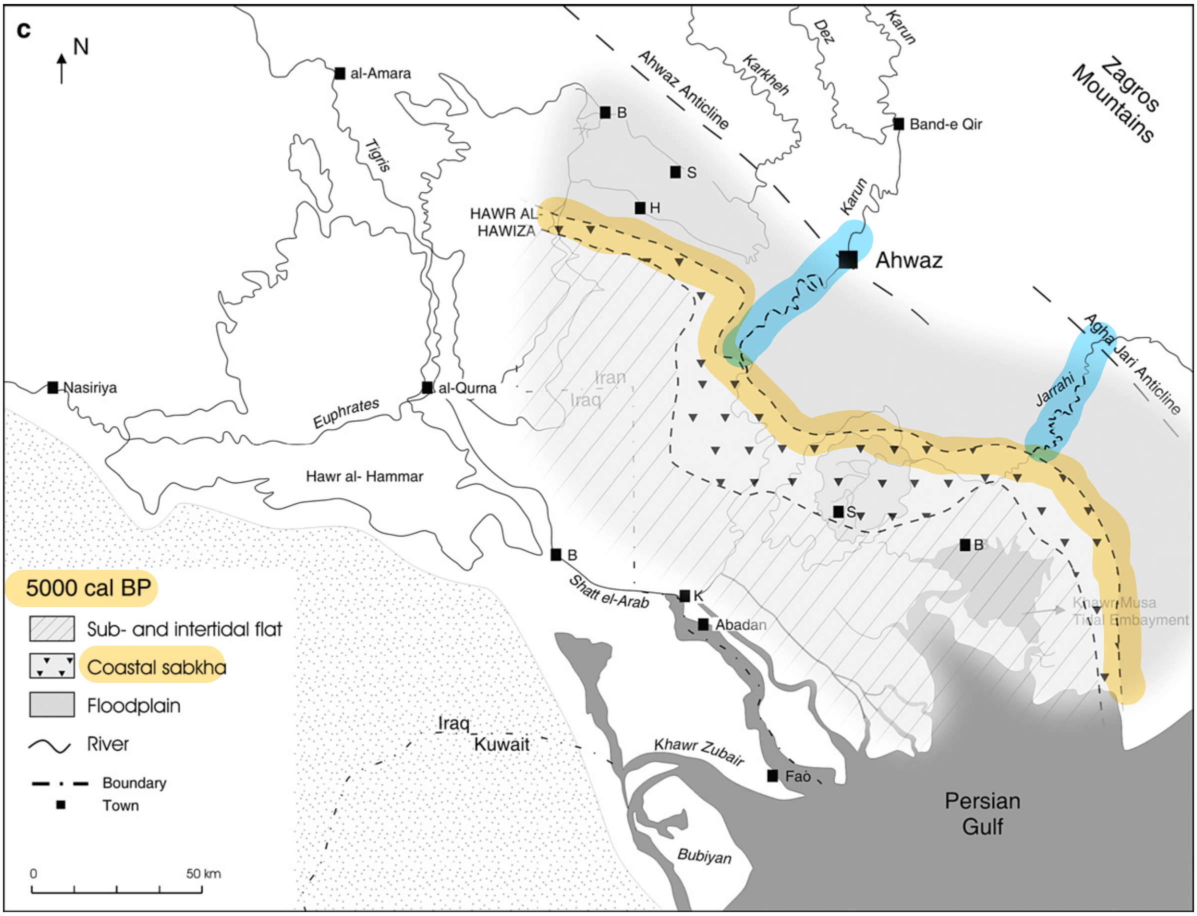

Fig. 11. Reconstruction of the environmental setting of the Lower Khuzestan plain around 5000 cal BP.

more important. Sabkhas were replaced by fluvial deposits and a brackish–freshwater marsh developed at ca. 350–430 cal BP. This date sets a minimum age for the formation of the distributary system of the Jarrahi river.

6. Discussion and conclusion

6.1. Palaeogeography of the plain

With 15 radiocarbon-dated samples available, any attempt to describe the palaeogeographic evolution of the Lower Khuzestan plain is constrained by the assumptions behind the reconstructions that are used to interpolate between dated samples through both time and space. The paucity of data makes it very difficult to define the extent of different environments, even in general. Moreover, the development of a coastal plain is a function of the following factors: rate of relative sea-level rise, morphology of the flooded surface, sediment budget, and accommodation space (Baeteman, 1998; Beets and van der Spek, 2000). Exact data about these factors is not known. Therefore, the reconstructions presented below must be regarded as a broad scheme considering the large-scale evolution.

As mentioned above, a prerequisite for the reconstruction of the Holocene palaeogeography is a reliable model of the original morphology of the pre-transgressive surface. It is essential to know the location and the morphology of the river valleys and their drainage pattern. It is via these valleys that the sea invaded the area once the sea level started to rise in the Holocene. The relief of the pre-transgressive surface was largely formed during the late Pleistocene sea-level lowstand. For the study area, only the pre-transgressive surface in the very northern part (Zone 1) is rather well documented. The second prerequisite for a Holocene palaeogeographical reconstruction is the knowledge of the history of changes in relative sea level. The data available so far in the framework of this investigation are not sufficient to produce a sea-level curve. In the literature,

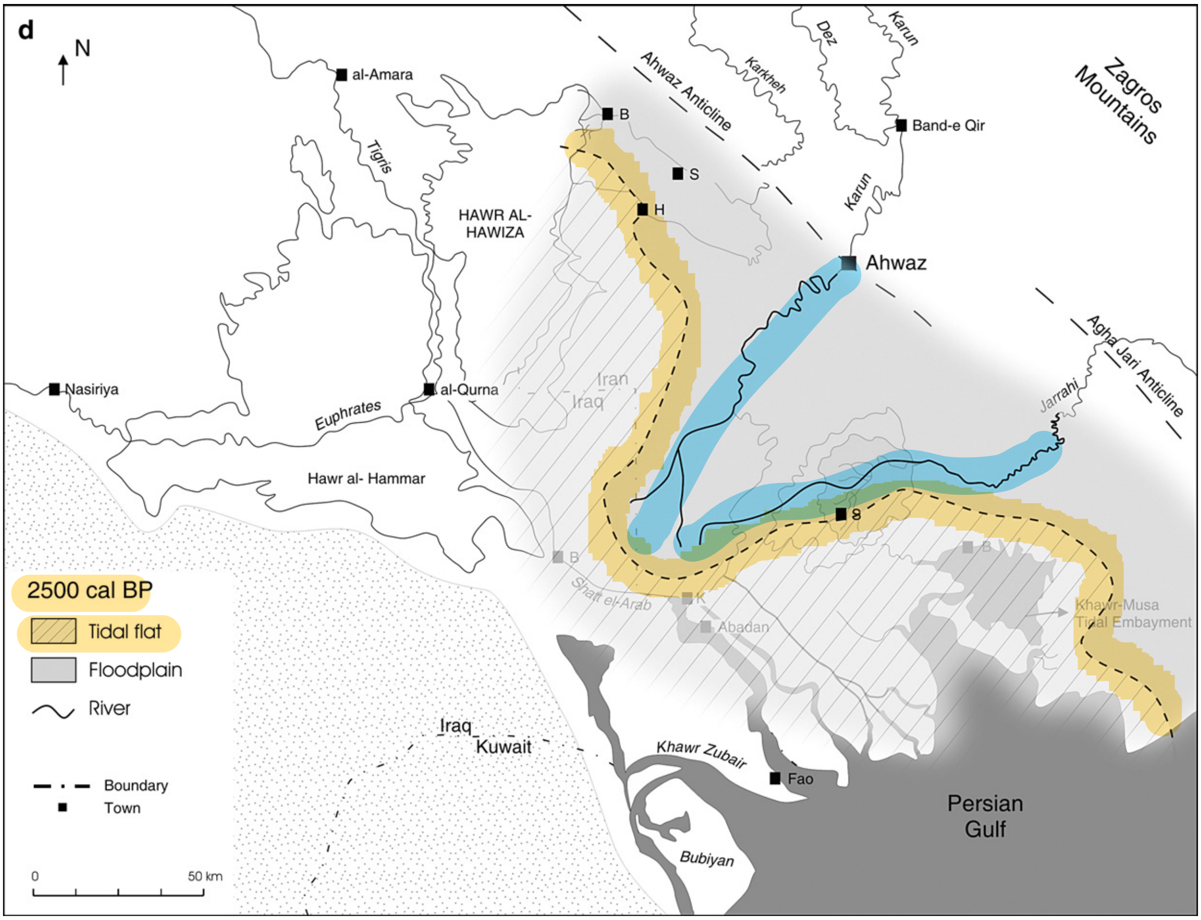

Fig. 11. Reconstruction of the environmental setting of the Lower Khuzestan plain around 2500 cal BP.

little is known about the post-glacial evolution of the sea level in the Persian Gulf. Only suspect data on sea-level evolution are available.

The approach adopted here for the palaeogeography is to use the reconstruction of past sedimentary environments from sediment cores and their relationship to tide levels. Changes in sedimentary environments at different locations through time reflect changes in the different locations of the estuaries and land–ocean boundary (shoreline) and the balance between fresh- and seawater inputs. Time estimates are inferred from the few dated levels. Consolidation and compaction of the sediments have not been taken into account. The upper 5 m of the sedimentary succession generally consists of a very compact clay. This clay consolidated shortly after deposition because of the high evaporation. Therefore, compaction of the deposits can be neglected to a great extent, except for the lower part of the sediment succession consisting of water-saturated sub- and intertidal deposits. This is in contrast with the findings of Aqrawi (1995), who stated that the greatest reduction in thickness caused by compaction occurs within the upper 2 to 5 m.

As discussed above, the Holocene sequence in general does not display a wide range of sediment types. For the reconstructions illustrated in Fig. 11 we show the following major environments: sub- and intertidal flats, coastal sabkhas, brackish–freshwater marshes and floodplains. For the two maps showing the reconstruction in the early Holocene, only tidal flats and floodplains are indicated, because a further differentiation is not justified given the data available. The different time slices are chosen according to the available radiocarbon dates and to some major changes in the development of the plain. The reconstruction of the palaeochannel belts of the rivers Karun, Karkheh and Jarrahi is based on the age model represented in Heyvaert and Weerts (submitted for publication).

Our results demonstrate a landward extension of the Gulf until at least 80 km north of its present-day shoreline at about 8000 cal BP (Fig. 11a). Due to a high

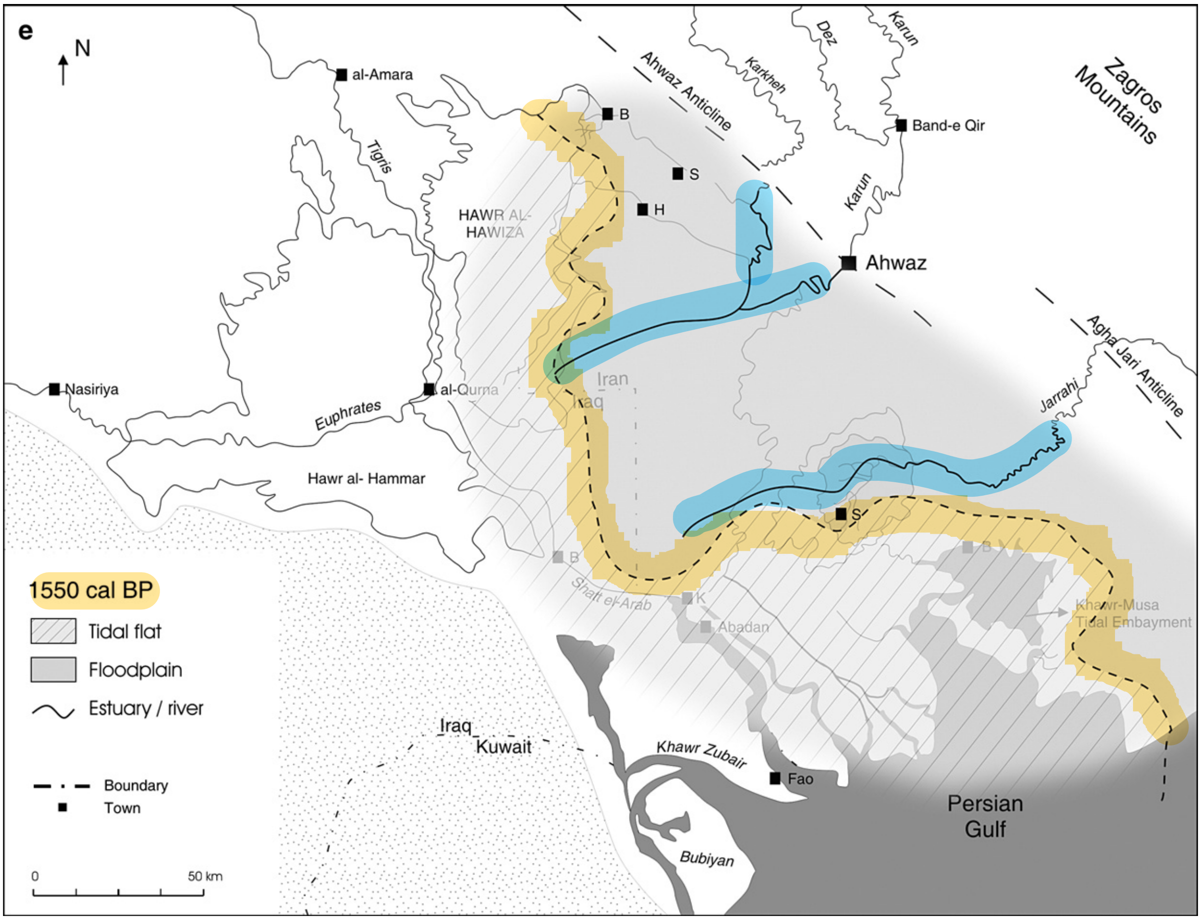

Fig. 11. Reconstruction of the environmental setting of the Lower Khuzestan plain around 1550 cal BP.

rate of RSL, the area was flooded rapidly and the tidal environments shifted landwards. Certainly until 7000 cal BP (Fig. 11b), the low lying areas were essentially wetlands on account of the proximity of the water table to the surface and/or their susceptibility to inundation by estuarine or riverine flooding and little evaporation. Salt marsh with reed growth developed, however, not for a time sufficiently long for peat to accumulate. This, together with the indication of various high intertidal silting-up phases with vegetation growth, indicate a high supply of coastal sediment and a rapid RSL rise.

From the sedimentary record it is obvious that this situation changed, but no radiocarbon age determinations relating to this transition are available. Instead of salt marshes, coastal sabkhas developed directly landwards of the high intertidal flat (Fig. 11c). The intersedimentary gypsum growth indicates that the deposition still happened in a high intertidal/supratidal environment and that the transition does not yet reflect a seaward progradation of the plain with less frequent (marine) flooding. The thin laminae of red-brown compact clay, the lack of biogenous traces and the abundance of evaporites are characteristics of a high evaporation (cf. Thompson, 1975) indicating a possible climatic change towards a more arid setting. Aqrawi (2001) found a similar transition in the Tigris–Euphrates plain, which he estimated to have taken place at approximately 4500 cal BP. It is suggested that deceleration of the RSL rise after approximately 5500 cal BP, together with more arid conditions, allowed coastal sabkhas to extend widely and aggradate while the position of the coastline remained relatively stable.

Continued deceleration of RSL rise initiated the progradation of the coastline from ca. 2500 cal BP (Fig. 11d). The effect of sediment supply by the rivers became more important than the effect of RSL rise. Major parts of the sabkhas were gradually replaced by a floodplain. Heyvaert and Weerts (submitted for publication) show that an avulsive-controlled Karun megafan developed. The avulsive shifting of the river Karun did not

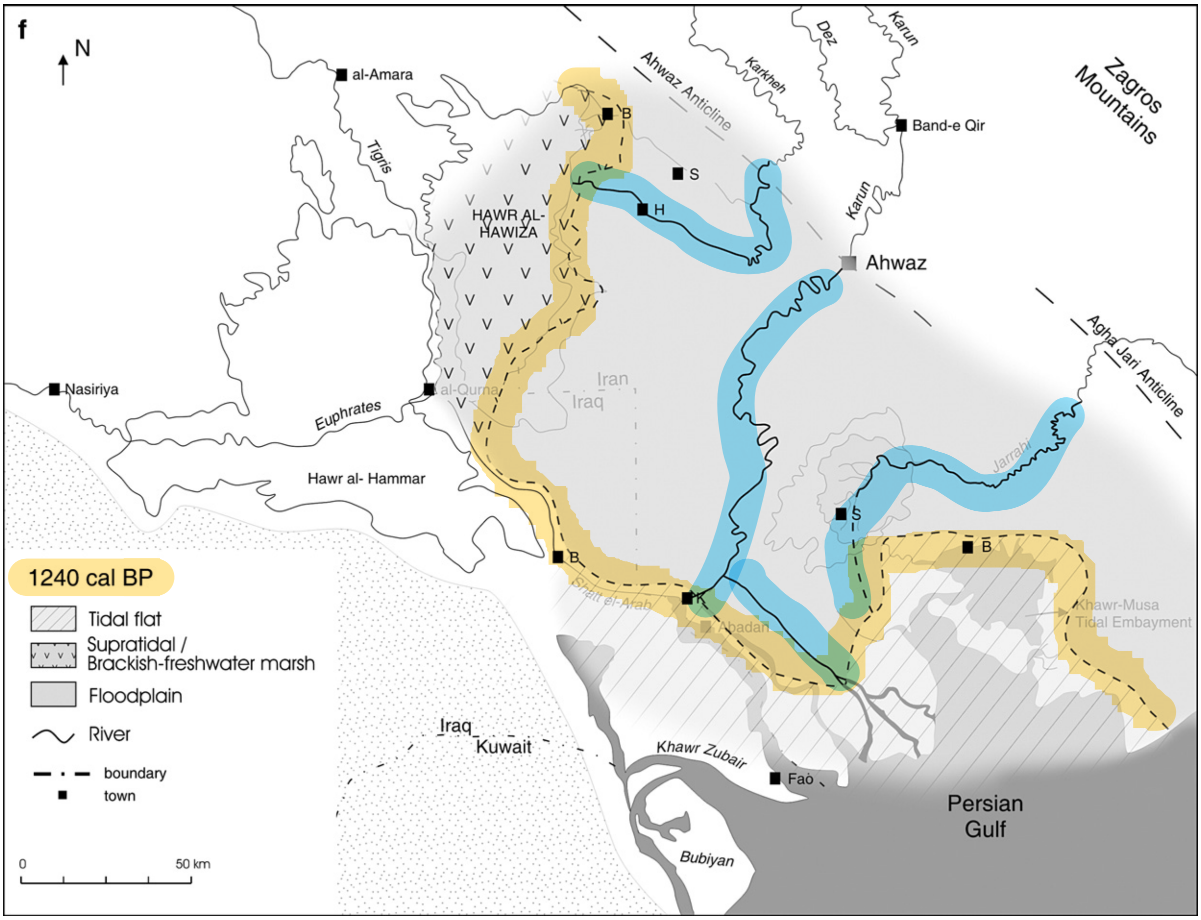

Fig. 11. Reconstruction of the environmental setting of the Lower Khuzestan plain around 1240 cal BP.

only determine the loci of fluvial sediment input by the river Karun, but also influenced the changing position of the Karkheh and Jarrahi channel and their loci of sediment input. By approximately 2500 cal BP, a palaeochannel belt of the river Karun and Jarrahi started to fill in the tidal environment in the southern part of the central plain. However, the tidal environment continued to expand in the northern part of the plain, which hitherto has been out of the reach of marine influence. Based on the age model for the palaeochannels (Heyvaert and Weerts, submitted for publication), we know that in the period between 2281 cal BP to 1240 cal BP, the Karun shifted north (Fig. 11e). The Karun avulsion belt complex started to reduce the initial width of the tidal embayment directly to the south of Qurna (Iraq). In the northern part of the plain, the tidal environment became isolated and changed gradually into a brackish–freshwater marsh environment. In the period between 1240–1000 cal BP (Fig. 11f) the Karun avulsed to its present-day position, and started to control the progradation of the coastline in the southern part of the plain. In the northern part of the plain, the brackish–freshwater marshes became locally filled up by the newly developed Karkheh palaeochannel nearby the village of Hawiza. By 450 cal BP (Fig. 11g), in the southern part of the plain, a brackish–freshwater marsh started to develop in the surroundings of the Jarrahi distributary system.

6.2. Implications of the palaeogeographical reconstruction for the Persian Gulf sea-level history

In this study, we do not possess enough accurate sea-level index points to produce a RSL curve. A general trend of decelerating RSL rise was observed. However, based on the sedimentary record and chronological data it can be proven that a Holocene RSL highstand, above present sea level, did not occur.

Near the present-day village of Bostan (Zone 1), located 200 km north of the present-day coastline, tidal deposits evolving into supratidal to brackish–freshwater deposits were found directly overlying the pre-

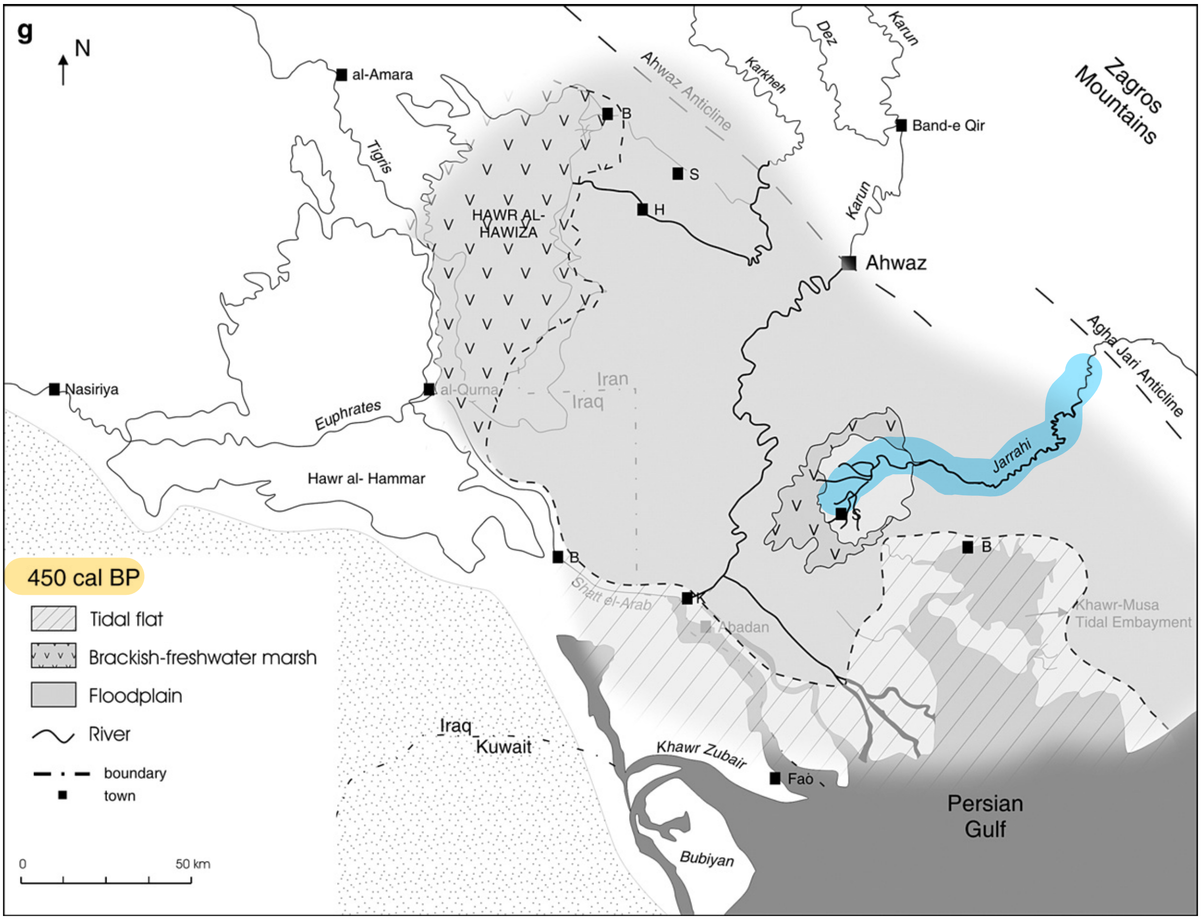

Fig. 11. Reconstruction of the environmental setting of the Lower Khuzestan plain around 450 cal BP.

transgressive surface at a level of +2 to +3.0 m (between MSL and MHHW, Figs. 3 and 4). At the earliest at 150 cal BP, the brackish–freshwater marsh became in filled by fluvial deposits (level +3.75 to +4 m, i.e. 2 m above present-day mean sea level).

The young age and the elevation of the tidal and brackish–freshwater deposits found on top of the pre-transgressive surface demonstrate that a sea-level high-stand around 6000 cal BP of 1 to 2 m above the present-day sea-level, as claimed by Dalongeville and Sanlaville (1987) did not occur. A higher RSL would have inundated the region of Bostan (Zone 1) as well, leaving behind tidal deposits with an age of ca. 6000 cal BP on top of the pre-transgressive surface. A RSL higher than the present one would have inundated also the southern regions of the Lower Khuzestan plain, leaving behind tidal deposits of that age at a level above present-day mean sea level. In none of the cores located to the south of Zone 1, this was recorded. Our data indicate also that a maximum lateral extension, as far as the city of Ahwaz around 6000 cal BP, as suggested by Sanlaville (1989, 2002) and Sanlaville and Dalongeville (2005), never existed. Moreover, these authors suggest also that the period after 6000 cal BP was marked by a gradual sea-level fall upon which some oscillations are superimposed. However, the sedimentary record of the Lower Khuzestan plain did not reveal evidence for a RSL fall, or transgressive/regressive sedimentary successions due to sea-level fluctuations.

This study shows that during the early and middle Holocene, the Lower Khuzestan plain was a low-energy tidal embayment under estuarine conditions. It is demonstrated that the sedimentary infill of this coastal embayment took place under a decelerating RSL rise, whereby the relative importance of controlling factors as sediment budget and accommodation space changed in the course of time. It is suggested that the Holocene development of the plain switched from retrogradational to aggradational and eventually to progradational. The late Holocene progradation of the coastline was determined by the interplay between fluvial sediment input, controlled by the development of a Karun megafan, and a decelerating rate of sea-level rise. The palaeogeographical reconstructions presented in this paper represent a significant step forward with respect to earlier reconstructions of the Lower Khuzestan plain and provide a framework for further research.

Acknowledgement

This research is funded by a grant from the Interuniversity Attraction Poles Programme — Belgian Science Policy. Mina Alizadeh, Beshad Askari, Dariush Baratvand and Abdol Reza Paymanu of the Iranian Culture Heritage Organization, Ahwaz, are thanked for their logistic support during the field surveys in January–February and December 2004. Mark Van Strydonck has provided the calibration of the radiocarbon datings. Dr. Henk Weerts is thanked for giving comments on earlier versions of this paper. Olivier Wambacq is thanked for the skilful production of the figures. Prof. H. Bruckner and an anonymous reviewer are thanked for their comments on this paper. This paper is a contribution to the IGCP Project 495 “Quaternary Land–Ocean Interactions: Driving Mechanisms and Coastal Responses” and to the INQUA Commission on Coastal and Marine Processes.

References

Admiralty Tide Tables, Volume 3, 2005. Indian Ocean and South China Sea, United Kingdom Hydrographic Office, 2004, Taunton, Somerset, UK.

Ainsworth, W., 1838. Researches in Assyria, Babylonia and Chaldea. John W. Parker, London.

Al-Azzawi, M., 1986. La sédimentation actuelle sur la plaine de la basse Mésopotamie, Irak, Unpublished PhD Thesis, University of Paris, Orsay.

Al-Zamel, A.Z., 1983. Geology and oceanography of recent sediments of Jazirat Bubiyan and Ras As-Sabiyah, Kuwait, Arabian Gulf, Unpublished PhD Thesis, University of Sheffield, UK.

Aqrawi, A.A.M., 1993. Recent sediments of the Tigris–Euphrates delta: the southern marshlands (Ahwar), Unpublished PhD Thesis, University of London, Imperial College of Science, Technology and Medicine, UK.

Aqrawi, A.A.M., 1995. Correction of Holocene sedimentation rates for mechanical compaction: the Tigris–Euphrates delta, lower Mesopotamia. Mar. Petrol. Geol. 12, 409–416.

Aqrawi, A.A.M., 2001. Stratigraphic signatures of climate change during the Holocene evolution of the Tigris–Euphrates delta, lower Mesopotama. Glob. Planet. Change 28, 267–283.

Aqrawi, A.A.M., Evans, G., 1994. Sedimentation in lakes and marshes (Ahwar) of the Tigris–Euphrates delta, southern Mesopotamia. Sedimentology 41, 755–776.

Audley-Charles, M., Curry, J., Evans, G., 1987. Location of major deltas. Geology 67, 175–197.

Baeteman, C., 1994. Subsidence in coastal lowlands due to groundwater withdrawal: the geological approach. J. Coast. Res. Special Issue 12, 61–75.

Baeteman, C., 1998. Factors controlling the depositional history of estuarine infill during the Holocene. Actas do 1° Simposio Interdisciplinar de Processos Estuarinos, Universidado do Algarve, Faro.

Baeteman, C., Dupin, L., Heyvaert, V.M.A., 2004/2005. Geo-environmental Investigation. In: Gasche, H. (Ed.), The Persian Gulf shorelines and the Karkheh,Karun, and Jarrahi Rivers: a geo-archaeological approach. Akkadica Offprint vol. 125/126, 155–215, 5–15.

Baltzer, F., Purser, B.H., 1990. Modern alluvial fan and deltaic sedimentation in a foreland tectonic setting: the lower Mesopotamian plains and the Arabian Gulf. Sediment. Geol. 67, 175–197.

Beets, D.J., van der Spek, A.J.F., 2000. The Holocene evolution of the barrier and the back-barrier basins of Belgium and the Netherlands as a function of late Weichselian morphology, relative sea-level rise and sediment supply. Geol. Mijnb. Neth. J. Geosci. 79, 3–16.

Beke, C.T., 1835. On the geological evidence of the advance of the land at the head of the Persian Gulf. Lond. Edinb. Philos. Mag. J. Sci. 3 (7), 40–46.

Dalongeville, R., 1990. Présentation physique générale de l'île de Failaka. In: Calvet, Y., Gachet, J. (Eds.), Failaka. Fouilles françaises 1986–1988. Traveaux de la Maison Orient, Lyon, pp. 23–40.

Dalongeville, R., Sanlaville, P., 1987. Confrontations des datations isotopiques aux données géomorphologique et archéologiques à propos des variations relatives du niveau marin sur la rive arabe du Golfe Persique. In: Aurenche, O., Evin, J., Hours, F. (Eds.), Chronologies in the Near East, Relative Chronologies and Absolute Chronology 16000–4000 BP, Colloque international du CNRS, BAR International Series 379. Archaeological series 3, Oxford-Lyon, pp. 567–584.

Dalongeville, R., Bernier, P., Dupuis, B., 1993. Les variations récentes de la ligne de rivage dans le Golfe Persique. Bulletin de l'Institut Geologique du Bassin d'Aquitaine, 179–192.

De Morgan, J., 1900. Etude géographique sur la Susiane. Rech. Archéol. Mém. 1, 448–460.

Einsele, G., 1992. Sedimentary Basins. Evolution, Facies, and Sediment Budget. Springer Verlag, Berlin.

Evans, G., 1979. The development of the Mesopotamian delta, comments. Geogr. J. 145, 529–531.

Falkenstein, A., 1951. Die Eridu Hymme. Sumer 7, 198–203.

Gunatilaka, A., 1986. Kuwait and the Northern Arabian Gulf: a study on Quaternary sedimentation. Episodes 9, 223–231.

Hansman, J.F., 1978. The Mesopotamian delta in the first millennium. Geogr. J. 144, 49–61.

Haynes, S.J., McQuillan, H., 1974. Evolution of the Zagros suture zone. Geol. Soc. Amer. Bull. 85, 739–744.

Heyvaert, V.M.A., Dawson, S., Sharma, C., submitted for publication. Facies interpretation of the Holocene sedimentary sequence of the Lower Khuzestan plain (southwest Iran), Persian Gulf: a lithogenic-palaeoecologic approach. The Holocene.

Heyvaert, V.M.A., Weerts, H.J.T., submitted for publication. The development of the Holocene Karun megafan, Lower Khuzestan, southwest Iran. Sedimentary Geology.

Höpner, T., 1999. Intertidal treasure Khowr-e Mussa — unraised. Wadden Sea Newsl. 1, 3–5.

Hudson, R.G.S., Eames, F.E., Wilkins, G.L., 1957. The fauna of some recent marine deposits near Basrah, Iraq. Geol. Mag. 94, 393–401.

Jacobsen, T., 1960. The waters of Ur. Iraq 22, 174–185.

James, G.A., Wynd, J.G., 1965. Stratigraphic nomenclature of Iranian oil consortium agreement area. Bull. Am. Assoc. Petrol. Geol. 49, 2182–2245.

Lambeck, K., 1996. Shoreline reconstructions for the Persian Gulf since the last glacial maximum. Earth Planet. Sci. Lett. 142, 43–57.

Le Strange, G., 1905. The Lands of the eastern Caliphate, Mesopotamia, Persia and Central Asia from conquest to the time of Timur. Cambridge University Press.

Larsen, C.E., 1975. The Mesopotamian delta region: a reconsideration of Lees and Falcon. J. Am. Orient. Soc. 95, 43–57.

Larsen, C.E., Evans, G., 1978. The Holocene geological history of the Tigris–Euphrates–Karun delta. In: Price, W.C. (Ed.), The Environmental History of the Near and Middle East. Academic Press, London, pp. 227–244.

Lees, G.M., Falcon, N.L., 1952. The geographical history of the Mesopotamian plains. Geogr. J. 118, 24–39.

Macfadyen, W.A., Vita-Finzi, C., 1978. Mesopotamia: the Tigris–Euphrates delta and its Holocene Hammar fauna. Geol. Mag. 115, 287–300.

Macleod, J.H., 1969. Geological Map of Ahwaz. Sheet 20829 E, scale 1:100.000. Iranian oil operating companies, Geological and Exploration Division, Teheran.

Mook, W.G., Steurman, H.J., 1983. Physical and chemical aspects of radiocarbon dating. Proceedings of the First International Symposium ^{14}C and Archeology. Groningen, 1981, PACT, vol. 8, pp. 31–55.

Morhange, C., Laborel, J., Laborel-Deguen, F., 1998. Précision des mésures de variations relative verticale du niveau marin à partir d'indicateurs biologiques. Le cas des soulèvements badysismiques de Pouzzoles, Italie du Sud (1969–1972; 1982–1984). Z. Geomorphol. 42, 143–157.

Purser, B.H., 1973. The Persian Gulf, Holocene Carbonate Sedimentation and Diagenesis in a Shallow Epicontinental Sea. Springer Verlag, Berlin.

Purser, B.H., Ya'acoub, S.Y., Al-Hassni, N.H., Al-Azzawi, M., Orzag-Sperber, F., Hassan, K.M., Plaziat, J.C., Younis, W.R., 1982. Charactères et évolution du complexe deltaique Tigre–Euphrate. Mém. Soc. Géol. Fr. 144, 207–216.

Plaziat, J.C., Younis, W.R., 1987. The brackish and freshwater mollusks of southern Iraq and their ecological significance for the Quaternary evolution of the lower Mesopotamian plain. Conf. on Quaternary Sediments in the Arabian Gulf and the Mesopotamian Region, Kuwait.

Rzoska, J., 1980. Euphrates and Tigris, Mesopotamian ecology and density. In: Illiesled, J. (Ed.), Monographiae Biologicae, vol. 38. The Hague, London.

Saleh, A., Al-Ruwaih, F., Al-Reda, A., Gunatilaka, A., 1999. A reconnaissance study of a clastic coastal sabkha in Northern Kuwait, Arabian Gulf. J. Arid Environ. 43, 1–19.

Sanlaville, P., 1989. Considération sur l'évolution de la basse Mésopotamie au cours des derniers millénaires. Paléorient 15, 5–27.

Sanlaville, P., 2002. The deltaic complex of the lower Mesopotamian plain and its evolution through millennia. In: Nicholson, E., Clark, P. (Eds.), The Iraqi Marshlands. Politico's Publishing, London, pp. 133–150.

Sanlaville, P., Dalongeville, R., 2005. L'évolution des espaces littoraux du Golfe Persique et du Golfe d'Oman depuis la Phase finale de la transgression post-glaciaire. Paléorient 31, 9–26.

Sanlaville, P., Dalongeville, R., Evin, J., Paskoff, R., 1987. Modification du trace littoral sur la côte Arabe du Golfe Persique en relation avec l'archeologie. In: Deplacement des lignes de rivage en Mediterané. Paris, pp. 211–222.

Setudehnia, A., O'B Perry, J.T., 1966. Geological map of Agha Jari. Sheet 20835 E, scale 1:100,000. Iranian oil operating companies, Geological and Exploration Division, Teheran.

Stuiver, M., Reimer, P.J., 1993. Extended ^{14}C data base and revised CALIB 3.0 ^{14}C age calibration. Radiocarbon 35, 215–230.

Thompson, R.W., 1975. Tidal-flat sediments of the Colorado River delta, Northwestern Gulf of California. In: Ginsburg, R.N. (Ed.), Tidal Deposits. Springer Verlag, New York, pp. 57–65.

Törnqvist, T.E., De Jong, A.F.M., Oosterbaan, W.A., Van der Borg, K., 1992. Accurate dating of organic deposits by AMS ^{14}C measurement of macrofossils. Radiocarbon 34, 566–577.

Ya'acoub, S.Y., Purser, B.H., Al-Hassni, N.H., Al-Azzawi, M., Orzag-Sperber, F., Hassan, K.M., Plaziat, J.C., Younis, W.R., 1981. Preliminary study of the Quaternary sediments of SE Iraq. Joint-project between the Geological Survey of Iraq and University of Paris XI, Orsay, Unpublished report.

Vita-Finzi, C., 1979. Rates of Holocene folding in the coastal Zagros near Bandar Abbas, Iran. Nature 278, 632–634.